Master's thesis

NTNU
Norwegian University of Science and Technology
Faculty of Medicine and Health Sciences
Kavli Institute for Systems Neuroscience

Liv Støldal Nielsen

Characterizing the newly generated CamKIIα-*Tdg*$^{-/-}$ mouse model

Master's thesis in Neuroscience
Supervisor: Jing Ye
Co-supervisor: Magnar Bjørås
May 2023

NTNU
Norwegian University of
Science and Technology

Liv Støldal Nielsen

Characterizing the newly generated CamKIIα-*Tdg*$^{-/-}$ mouse model

Master's thesis in Neuroscience
Supervisor: Jing Ye
Co-supervisor: Magnar Bjørås
May 2023

Norwegian University of Science and Technology
Faculty of Medicine and Health Sciences
Kavli Institute for Systems Neuroscience

NTNU
Norwegian University of
Science and Technology

Abstract

Thymine DNA glycosylase (TDG) is an enzyme that plays an important role in genome repair through the removal of T/G mismatches. Recent evidence shows that TDG also has an active role in DNA demethylation, suggesting an additional role in transcriptional regulation. This is because DNA methylation hinders the binding of the transcriptional machinery and can recruit gene repression proteins. This leads to gene suppression, while DNA demethylation is associated with gene expression. As regulation of DNA methylation pattern is thought to be involved in transcriptional mechanisms essential for long-term memory, we questioned whether TDG-mediated DNA demethylation would be involved in the formation of long-term memory. In this study, the conditional knockout mouse model CamKIIα-*Tdg*$^{-/-}$ was used to investigate whether TDG depletion in hippocampal neurons led to alterations or impairments in long-term memory. Firstly, by using immunohistochemistry, I confirmed the Cre-induced GFP expression and presumably Cre-induced-*Tdg* knockout in all three hippocampal regions (CA1, CA3, and DG). Further, I assessed spatial memory of adult male CamKIIα-*Tdg*$^{-/-}$ and LoxP-mini*Tdg* (control) mice using the established novelty preference tests Novel Object Location (NOL) and Y-maze, as well as the anxiety levels using the Open Field Test (OFT). In addition, anxiety and spatial memory were assessed in young (4-month-old) and aged (18-19-month-old) LoxP-mini*Tdg* control mice. Lastly, I optimized the behaviour protocols to reduce stress in animals, make the procedure more time-efficient, and increase the interest of animals in the exploration of the novel and familiar right arm in the Y-maze. My findings suggest that: 1) the majority of *Tdg* knockout occurs in the CA1, with over 80% of the neurons being GFP positive, though we also observe extensive GFP expression and presumable TDG depletion in CA3 and DG, suggesting consistent TDG depletion in the hippocampus. 2) Though some indication of less novelty preference in CamKIIα-*Tdg*$^{-/-}$ animals compared to the control group was observed, the difference was not significant, and more animals are needed to show statistical difference. It is therefore not clear whether TDG depletion in hippocampal neurons affects spatial memory. 3) We observed that the aged LoxP-mini*Tdg* mice showed some indication of less novelty preference than the young control group indicating impairment in spatial memory, though more animals need to be added to increase reliability. 4) The optimization of the protocol successfully implemented the use of red tunnels to transport mice from cage to maze and reduced the Y-maze habituation sessions. In addition, there were some indications of increased exploratory activity to the right and novel arm, though more animals need to be added to increase reliability.

Sammendrag

Tymin DNA glycosilase (TDG) er et enzym som har en viktig rolle i genom reparasjon via fjerningen av T/G uoverensstemmelser. Nyere forskning viser at TDG også har en aktiv rolle i DNA demetylering, noe som tilsier at den og har en rolle i regulering av gen-transskripsjon. Dette er fordi DNA metylering forhindrer bindingen av det transkripsjonelle maskineriet, og kan rekruttere proteiner involvert i genundertrykkelse. Dette fører til genslukking, mens DNA demetylering er assosiert med genuttrykk. Fordi man tror at regulering av DNA metyleringsmønstre er involvert i transkriberings-mekanismer som er essensielle for langtidshukommelse, kan man spørre seg om TDG mediert DNA demetylering er involvert i dannelsen av langtidshukommelse. Denne studien bruker den betingede musemodellen CamKIIα-*Tdg*$^{-/-}$ for å undersøke om «knockout» av TDG i nevroner i hippokampus fører til endringer eller svekkelse av langtidshukommelse. Jeg brukte immunohistokjemi til å bekrefte Cre-indusert GFP uttrykkelse og antagelig Cre-indusert fjerning av *Tdg* i alle tre hippokampale regioner (CA1, CA3, DG). Videre evaluerte jeg stedshukommelsen til fullvoksne mannlige CamKIIα-*Tdg*$^{-/-}$ og LoxP-mini*Tdg* (kontroll) mus ved bruk av etablerte preferansetestene NOL og Y-maze, i tillegg til å måle frykt ved bruk av OFT. I tillegg ble frykt og stedshukommelse vurdert i unge (4 måneder gamle) og eldre (18-19 måneder gamle) LoxP-mini*Tdg* kontroll mus. Til sist optimaliserte jeg adferds-protokollene for å redusere påført stress, redusere tidsbruk, og øke musenes interesse i å utforske den ukjente venstre of kjente høyrearmen i Y-maze. Mine funn tyder på at: 1) Majoriteten av *Tdg* «knockout» skjer i CA1, hvor over 80% av nevronene er GFP positive, men vi observerer også omfattende GFP uttrykk og antagelig fjerning av *Tdg* i CA3 og DG, noe som indikerer jevn fjerning av TDG i hippokampus. 2) Selv om vi observerte noe indikasjon i nedgang av preferanse til det ukjente i CamKIIα-*Tdg*$^{-/-}$ mus sammenlignet med kontroll gruppen, så var differansen ikke signifikant, og inkludering av flere dyr i testene trengs for å vise statistisk differanse. Det er derfor ikke tydelig om fjerning av TDG i nevroner i hippokampus påvirker stedshukommelse. 3) Vi observerte at den eldre gruppen av LoxP-mini*Tdg* musene viste noen indikasjoner på mindre preferanse til det ukjente sammenlignet med den yngre kontroll gruppen, men flere dyr må bli inkludert i testene for å øke testens pålitelighet. 4) Optimalisering av protokollen førte til vellykket inkludering av røde tuneller til transportering av mus fra bur til labyrint, og reduserte antall tilvenningsøkter brukt i Y-maze. I tillegg så vi noen indikasjoner på økt utforskningsaktivitet til høyre of ukjent arm, men inkludering av flere dyr i testen trengs for å øke reliabiliteten.

Acknowledgements

I would like to express my gratitude to all the people that have helped me throughout this process. First, I would like to thank my main supervisor, Jing Ye, for allowing me to join this interesting project. I would also like to thank her for continuous supervision throughout my time in the group, as well as allowing me to work independently. Secondly, I want to thank my co-supervisor Magnar Bjørås for the resources making this project possible. I would also like to thank the rest of the members in the research group for all the interesting input and discussions we have had. I would like to especially thank Dagny Sanden Døskeland, who taught me most of the experimental methods used in this project, as well as reading my thesis and providing me with constructive criticism. I could not have done this without her. In addition, I would like to thank Vidar Langseth Saasen for helping out with the statistics and giving me feedback on the results section, Maria Cámara Quílez for helping me use Axioscan, and Marion Silvana Fernandez Berrocal for always being available for questions. I would also like to thank Karoline Opsahl for helping with some of the behavioural tests, and Nils Hagen for helping out at the Animal Facility. Lastly, I would like to thank my family and friends for all the support they have given me throughout my course of study.

Table of Contents

List of Figures

List of Tables

List of Abbreviations

5caC	5-CarboxylCytosine
5fC	5-FormylCytosine
5hmC	5-hydroxy-MethylCytosine
5hmU	5-HydroxyMethyl-Uracil
5mC	5-MethylCytosine
AID	Activation-induced Cytidine Deaminase
APE I	Apurinic/apyrimidinic Endonuclease I
APOBEC	Apolipoprotein B mRNA-editing Enzyme Complex
BDNF	Brain-Derived Neurotropic Factor
BER	Base Excision Repair

C	Cytosine
CA	Cornu Ammonis
CamKIIα	Calcium/Calmodulin-dependent protein kinase II alpha
CNS	Central Nervous System
DG	Dentate Gyrus
DNMT	DNA Methyltransferase
EC	Entorhinal Cortex
eGFP	Enhanced GFP
FACS	Fluorescence-Activated Cell sorting
FOTS	Forsøksdyrforvaltningens tilsyns- og søknadssystem
G	Guanine
GFP	Green Fluorescent Protein
HPC	Hippocampus
IHC	Immunohistochemistry
KO	Knockout
LTM	Long-Term Memory
M	Mean
NeuN	Neuronal Nuclear Antigen
NOL	Novel Object Location
NS	Nonsignificant
ns	Not significant
OF	Open Field
p29	Postnatal day 29
PCR	Polymerase Chain Reaction
RC	Release Corner
SD	Standard Deviation
STM	Short-Term Memory
T	Thymine
TDG	Thymine DNA Glycosylase
TET	Ten-Eleven Translocase
U	Uracil
WB	Western Blot
WT	Wild Type

1 Introduction

This introduction first shortly describes the role and functions of the enzyme Thymine DNA Glycosilase (TDG), and introduces TDGs role in the establishment of DNA methylation patterns in the genome. Further, the possible role of TDG in epigenetic regulation is introduced, and a description of the process of epigenetic regulation involving DNA methylation and demethylation, and its role in learning and memory. This is done so that the reader better understands the importance of studying enzymes like TDG that regulate the DNA methylation pattern, as this process regulates transcription of genes with roles in synaptic plasticity and memory formation (1). Next, the structure and function of the hippocampus is introduced, as it plays an imporant role in memory formation (2). As this study wanted to assess the role of TDG in hippocampal-dependent memory formation, the methods used for this assessment are then introduced. Behavioural tasks used to assess functional memory is introduced, followed by how conditional gene knockout is used to investigate tissue and time specific gene function.

1.1 Thymine DNA glycosylase

Thymine DNA glycosylase (TDG) is an enzyme with crucial functions in genome repair, transcriptional regulation, and epigenetic regulation (3,4). DNA methylation and demethylation are important mechanisms in epigenetic regulation, as hypermethylation in promoter regions is associated with gene silencing, and hypomethylation with gene expression (5). Interestingly, dynamic regulation of the methylation patterns has been implicated as a necessary mechanism in memory formation, due to its function in regulation of transcription of genes associated with synaptic plasticity (6). Because of TDG's role in DNA demethylation (7), it is feasible that TDG is implicated in the formation of long term memory (LTM).

TDG was originally discovered due to its functional role in repair of T·G mismatches in the genome (8). T/G mismatches are instances where a thymine (T) or uracil (U), is paired with a guanine (G) instead of cytosine (C), (9,10). These inaccurate pairs occur when cytosine or 5-methylcytosine (5mC) go through spontaneous hydrolytic deamination (9). The mismatch can lead to possible genetic changes due to the ambiguity of the G·T pairing, and the epigenetic information stored in the methyl group of 5-meC might be lost (11). By hydrolysing the N-glycosidic bond of T or U when it is coupled with G, the mis-paired base is excised, creating an abasic site (12,13). TDG further initiates repair of the abasic site by recruiting base excision repair (BER) associated proteins. Apurinic/apyrimidinic endonuclease I (APE I) cleaves the abasic site into a single nucleotide gap, generating a 3' hydroxy group. DNA polymerase B then fills the gap and a ligase complex seal the nick, completing the repair (14,15). In the end, the 5mC has been replaced with an unmethylated cytosine (12).

TDG also has direct functions in gene expression regulation through its interaction with transcription factors (4). TDG has been shown to interact with CREB binding protein, a coactivator that initiates transcription activation through chromatin remodelling (16). In addition, TDG plays a role in gene regulation through its role in the demethylation pathway.

After a spontaneous deamination of 5mC to a T, TDG can excise T and initiate BER, leading to the reinstating of an unmodified C. In addition, TDG is implicated in the oxidative TET pathway, as it can excise the oxidative derivates from ten-eleven translocase (TET) activity (17), completing the demethylation process.

TDG exhibits high activity in sites of the DNA with high concentrations of C·G base pairs, referred to as CpG sites (8,18). Hypomethylation of CpG sites in promotor regions are associated with gene expression. However, hypermethylation in promoter regions is associated with gene silencing (19). Through its function in DNA demethylation, TDG can indirectly regulate gene expression through epigenetic regulation.

Conventional knockout of the *Tdg* gene in mice is embryonically lethal, with the lethality occurring at age E11.5 (20–22). Fibroblasts derived from said embryos show that the genetic regulation has been impaired, and that the affected genes have imbalanced histone modification and CpG methylation (21). This shows that TDG has essential functions in regulation of genes that are important for embryonic development. Based on this evidence, it is pertinent to assume that the activity of TDG is linked to not only DNA repair, but also epigenetic modifications of DNA and regulation of gene expression.

1.1.1 TDG protein and gene

The *TDG* gene is located in chromosome 12, 23.3, (NCBI Gene ID:6996) in humans. It consists of a coding region of 3551 nucleotides, with the full length protein coded for by 10 exons (23). The full length TDG protein is 410 amino acids in length, and has an α/β structural conformation (24,25). TDG is part of the uracil glycosylase superfamily of DNA repair enzymes known to recognise and excise mismatched bases, more specifically U and T (21). There is ubiquitous expression of *Tdg* in several tissues in humans. According to the protein atlas, there is an intracellular general nuclear expression of *Tdg*, but low tissue specificity (26). In addition, *Tdg* is strongly expressed in neurons, and less so in glial cells (26). The glycosylase domain, which is the catalytic domain in TDG, modulates the enzymatic activity of TDG, and mediates interactions with proteins like transcriptional factors and nuclear receptors (27–29). The TDG ortholog in *Mus musculus* (*Tdg*) is located at 10C1; 10 39.72 cM (NCBI gene ID: 21665) (30). This is fortunate, as it makes it possible to use a mouse model when studying the role and function of TDG.

1.2 Epigenetic regulation by DNA methylation and demethylation

1.2.1 Epigenetics

Epigenetic mechanisms enable cellular diversity despite all cells sharing the same DNA. Epigenetic mechanisms like DNA methylation and histone modification can silence certain genes while activating others, allowing for functional difference and cell specificity. By regulating genome packaging, activating/deactivating transcription factors, and making dynamic covalent modifications to histones and DNA, cells have the ability to regulate the gene expression in response to changes in the environment (31). The epigenetic changes are inheritable, even though the changes are not found in the DNA sequence (32). Impairments of epigenetic mechanisms have been linked to various diseases like schizophrenia, Rett syndrome, and cancer (33,34). DNA methylation is one such epigenetic mechanism, and is involved in transcriptional regulation (35).

1.2.2 DNA methylation

DNA methylation is an epigenetic mechanism that involves direct chemical modification to the DNA, without altering the genetic sequence (35). The chemical modification involves the addition of a methyl group at the fifth carbon of a cytosine, a process catalysed by DNA methyltransferases (DNMT) (36). This addition creates steric hindrance and prevents the transcriptional machinery from having access to the promoter (37). In addition, it can also lead to the recruitment of transcription repressor factors (35). All of this prevents gene transcription (35,38–40).

De novo methylation is a type of DNA methylation where methyl groups are added to cytosine on previously unmethylated DNA (figure 1a), a process that primarily occurs during embryogenesis (41). This process is catalysed by DNMT3a and DNMT3b which are *de novo* DNMTs (42,43). DNMT1 is required for the maintenance of the methylation pattern in the genome, by recognising hemi-methylated DNA in the daughter strands, and restores the symmetrically methylation pattern in accordance with the mother strand after replication of the DNA (figure 1b) (35,44).

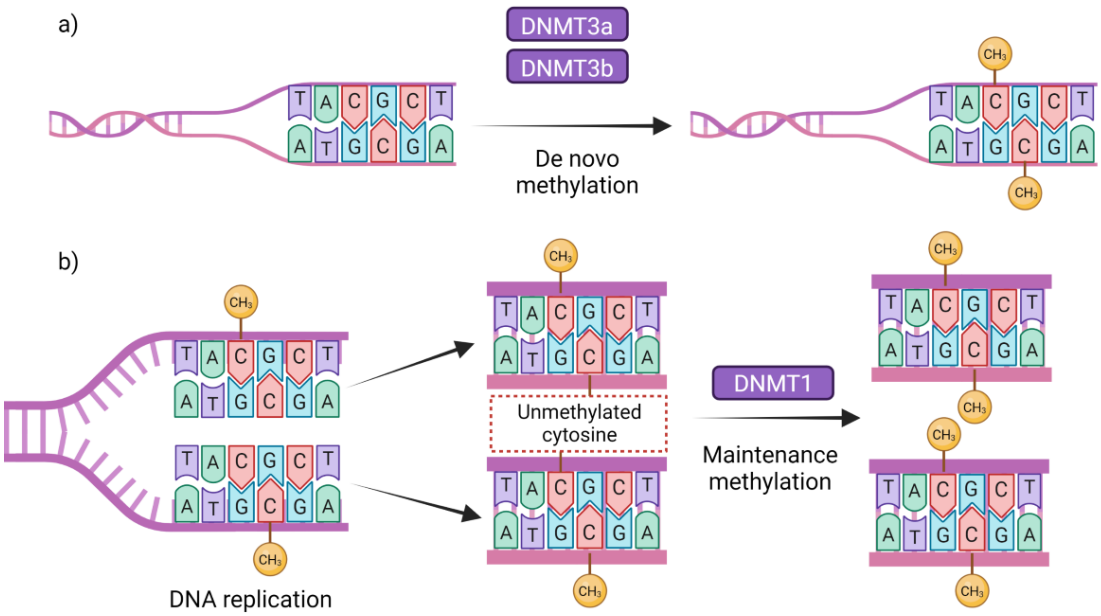

Figure 1. De novo methylation and maintenance methylation of DNA by DNMT3a, DNMT3b, and DNMT1. a) The figure depicts how the DNA methyltransferases DNMT3a and DNMT3b initially methylate unmethylated DNA via de novo methylation. b) The figure shows how DNMT1 restores the initial methylation pattern during maintenance methylation after DNA replication. The figure was created in Biorender.

1.2.3 DNA demethylation

Though DNA methylation patterns were long thought to be static after being established during embryonic development, later findings have shown that DNA methylation patterns are dynamic (45–47). The process of DNA demethylation is essential for the dynamic regulation of the methylation pattern. This process involves the removal of the methyl group of cytosine. We categorise DNA demethylation into two groups: active and passive DNA demethylation.

Passive DNA demethylation happens during replication when the daughter strand is not methylated by the maintenance methylation machinery of DNMT1, resulting in dilution of DNA methyl groups on the DNA strands for each replication round (35,44,48). Active demethylation describes the process where methyl groups are actively removed by a series of enzymes. 5mC can be modified at two sites: the amine group and the methyl group. Currently, there are several proposed mechanisms for demethylation, including 1) the pathway of spontaneous deamination of 5mC to T followed by base excision repair (BER) of the T·G mismatch, and 2) oxidation mediated demethylation by TET followed by BER (figure 2) (31,35,49).

The 5mC amine group can be spontaneously deaminated to a carbonyl group by a family of deaminases called AID/APOBEC (activation-induced cytidine deaminase/apolipoprotein B mRNA-editing enzyme complex) (50). This results in a T·G mismatch, which is repaired by TDG initiated BER (15,20,51) (figure 2). This process is called spontaneous deamination. Oxidation mediated demethylation is a process heavily catalysed by the TET enzymes. TET oxidises 5mC to 5-hydroxy-methylcytosine (5hmC), to 5-formylcytosine (5fC), and 5-carboxylcytosine (5caC) (52). 5hmC can be deaminated by AID/APOBEC, forming 5-hydroxymethyl-uracil (5hmU) (figure 2) (53). 5fC and 5caC are recognised and excised by TDG, followed by BER and restoration of the unmethylated cytosine (54). The many tasks of TDG in the different steps of demethylation suggests that TDG plays an important role in the regulation of methylation patterns in the DNA, and by extension, plays a role in transcriptional regulation.

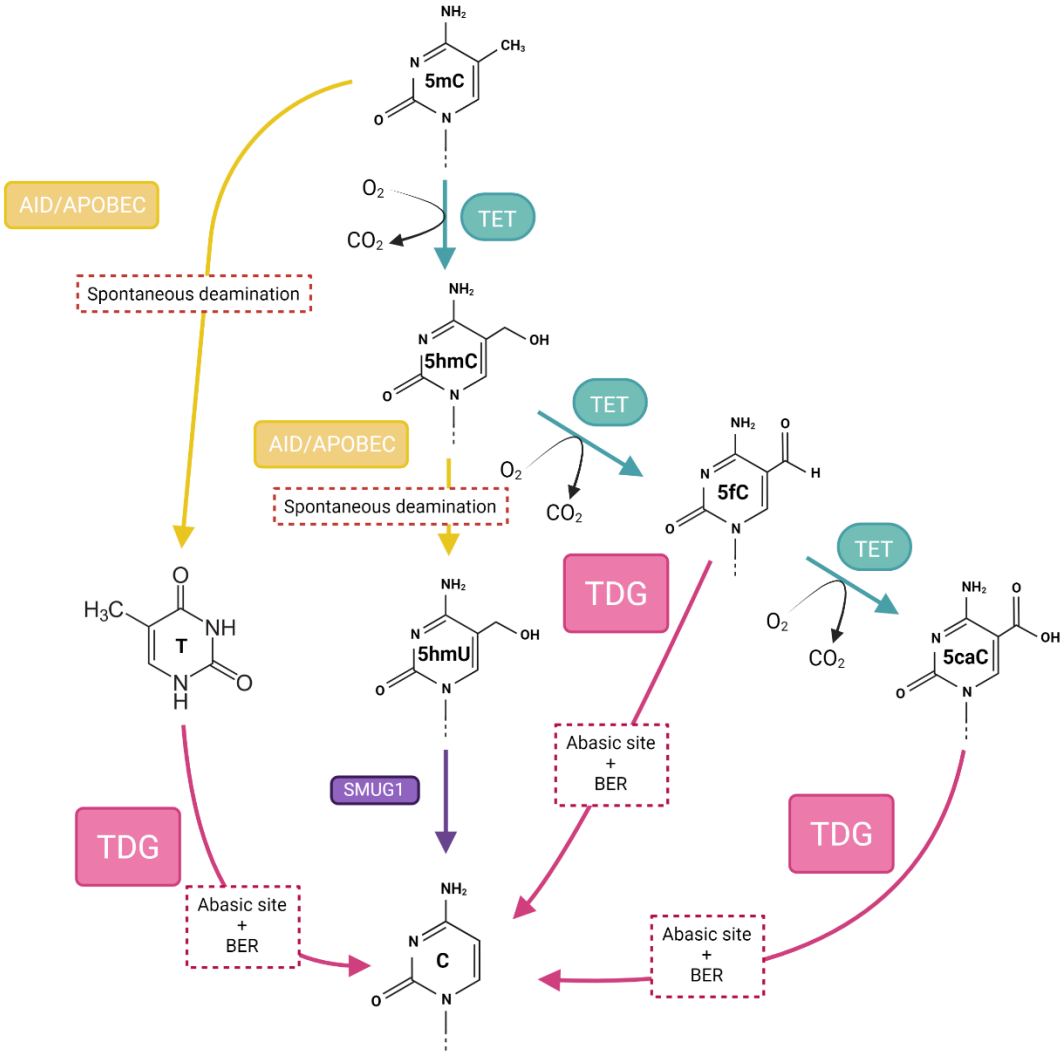

Figure 2. Active demethylation pathways involving TDG. The figure depicts the active demethylation of 5mC to C. 5mC is converted to T through spontaneous deamination, for then to be changed to cytosine through TDG initiated BER. In addition, 5mC is oxidised by TET to 5hmC, to 5fC, to 5caC through oxidation mediated demethylation. TDG recognises 5fC and 5caC and is changed to cytosine through BER.

1.2.4 DNA methylation and demethylation in learning and memory

As previously mentioned, DNA methylation is an important part in regulating gene expression through its interference with the transcription machinery and recruitment of proteins associated with gene repression (35,37). DNA methylation is thought to be an important component in both formation and storage of long term memory. This is supported by studies showing that there is dynamic regulation of the DNA methylation pattern in response to experience-related stimuli in the adult central nervous system (CNS) (55). Several studies have shown changes in regulation of genes associated with memory formation after activity induced changes in the methylation patterns. Martinowich et al. found that at the promotor of brain-derived neurotropic factor (BDNF), locus-specific demethylation has been reported to occur in neurons when stimulated (56). BDNF is a protein that is essential for adult neural plasticity. Lubin et al. saw that contextual fear learning induced differential regulation of exon-specific *bdnf* mRNAs (I, IV, VI, IX) that was associated with changes in *bdnf* DNA methylation (6).

Additionally, studies using genome-wide analysis have found that there is a change in the DNA methylation pattern after learning: Duke et al. showed that after applying contextual fear conditioning in rats, more than 5000 differentially methylated regions in the DNA had been induced in the hippocampal neuron genome (57). They observed that this led to about 500 genes being up-regulated and 1000 genes being downregulated in the rats. They also saw that there was an overall of 9.17% of genes in the genome of hippocampal neurons that were differently methylated than before the fear conditioning. Before Duke's study, Halder et al. had reported of DNA methylation changes specifically in the hippocampal CA1 region in mice after they had been through contextual fear conditioning (58). The findings of Duke and Halder support the theory that DNA methylation plays an important role in altering expression of genes involved in synaptic plasticity.

Levenson et al. showed that when inhibiting DNMT activity, not only will the DNA methylation pattern in the brain change, it will specifically change the DNA methylation of promotors associated with the plasticity promoting genes reelin and BDNF (59). This was followed up by Miller & Sweatt, who observed that rats treated with non-specific inhibitors of DNMTs showed impaired formation of memory related to contextual fear associations (60). This indicated that dynamic changes in DNA methylation is required for the formation of long-term memory. These findings further support the theory that DNA methylation and demethylation plays an important role in the expression of genes affiliated with learning, memory and plasticity. Furthermore, dysregulation of DNA methylation and demethylation processes is shown in neurological pathological conditions and cognitive decline associated with age, like drug addictions, neurodegenerative diseases, and psychiatric conditions (61–66). DNA methylation and gene expression seems to play a huge role in memory and learning, and when dysregulated it has a huge impact on our wellbeing. This further proves that understanding these processes are very important. To understand why methylation patterns in the hippocampus play such a huge role in learning and memory, we need to understand the role of the hippocampus in learning and memory.

1.3 The hippocampus

1.3.1 The anatomy and circuitry of the hippocampus

The hippocampus (HPC) is an important region in the brain of vertebrates (67). Located in the allocortex deep in the medial temporal lobe, the hippocampal formation consists of subregions that are classified based their connectivity to other regions, and their unique neuronal population (68,69). These subregions consist of hippocampus proper (Cornu ammonis, CA), which is further divided into CA1, CA2, CA3, and CA4, and dentate gyrus (DG), which is separated from CA by hippocampal sulcus as they curve into each other. Often included in the term hippocampal formation, are the regions of the entorhinal cortex (EC), which is connected to the HPC via the subiculum (70–72).

The HPC is connected to and receives sensory input from neocortical areas via the EC through the trisynaptic circuit, which plays an important role in conveying input related to sensory perception and spatial reasoning, enabling the acquisition of spatial and episodic memories (73–76). Through the perforant pathway, axons from the entorhinal cortex transmits input to the granule cells of DG (77,78). The trisynaptic circuit continues as DG transmits signals to the pyramidal signals in CA1 via mossy fibres, and the signal comes to a completion as CA3 signals to the pyramidal cells in CA1 through the Schaffer Collaterals (79,80). Signals form the CA1 area can exit the HPC and convey signals to other

brain regions via projections through the EC (81). Understanding the organisation of the hippocampal circuitry is important for the understanding of its function.

1.3.2 The hippocampus in learning and memory

The HPC plays an important role in the formation of long term episodic and spatial memories (82,83). Episodic memories refer to explicit declarative memories related to specific events in your life, while spatial memory refers to the ability to record and recover information about spatial location and is necessary for the ability to orient oneself in a space and to plan a course. Several studies have shown that lesions or other forms of damage in the hippocampal regions can lead to an impairment in learning and memory tasks related to spatial and episodic memory, demonstrating the important role the HPC plays in learning and memory (84–87). It is known that TDG is involved in demethylation, and that regulation of methylation patterns in the hippocampus is associated with learning and memory. A way to investigate if TDG activity has an effect on spatial memory is by performing tissue-specific knockout of *Tdg* in a mouse model. This could potentially lead to dysregulation of the DNA methylation pattern in HPC neurons, as well as impairment of spatial reference memory.

1.4 Using behavioural paradigms to assess spatial memory

Spatial memory can be assessed by using animal models and subjecting these animals to behavioural tasks designed for that purpose. Currently, there is a multitude of such established behaviour paradigms one can use to assess spatial memory in rodents, like the Y-maze, T-maze, radial arm maze, Morris water maze, Barnes maze, and novel object location (NOL). What these tests have in common, is that they measure an animal's ability to remember and recognise either an object or a location, thus assessing its functional spatial memory (88–93). The ability to navigate is linked to spatial memory, as learning and remembering new locations is crucial to this task. Allocentric navigation is the ability to use distal cues, that is, cues outside the organism, to locate oneself in the environment. This category of navigation involves the HPC and its surrounding structures. Egocentric navigation is the organism's ability to navigate based on internal cues (like speed and turns) (94). Several studies show that animals with knockout of genes associated with memory show an impaired performance in memory tasks (95–97). It is safe to assume that it is possible to assess the effect a gene/protein has on spatial memory and navigation by performing gene knockout and have the animals do certain behaviour tests to investigate if there is an impairment in performance.

1.5 Gene knockout in transgenic mice as a way of investigating gene function

1.5.1 Conditional gene knockout

By performing gene knockout, then subsequently monitoring phenotype changes in the animal, it is possible to determine the role/function of the gene in question. Conventional gene knockout, which is where knockout of the gene occurs in all cells in the animal, can lead to embryonic lethality if the gene in question is important for embryonic development and/or other viable processes (98). This obstacle makes it difficult to study gene function in adult animals. This issue can be solved by performing a conditional gene knockout. In this case, the knockout is both time and tissue specific, making it possible to study tissue specific functions of the gene of interest in adult animals (98). Several techniques for conditional knockout have been developed, one of them being the Cre-LoxP technique.

1.5.2 The Cre-LoxP system

Cre recombinase is a tyrosine specific recombinase derived from the P1 bacteriophage that recognises specific sites, *LoxP* sites, mediating deletion of the DNA in between two *LoxP* sites (98). In this way, it can be used to facilitate gene knockout when the gene of interest is in between *LoxP* sites. One *LoxP* site is a 34 bp sequence consisting of two 13 bp inverted and palindromic repeats and one 8 bp core sequence. The *LoxP* sites are introduced to an animal's genome through homologous recombination, flanking the gene of interest in the same direction (99,100). When Cre is introduced, it will excise the floxed gene, causing a deletion. Cre can be introduced to the tissue via viral gene delivery methods, or by breeding animals with floxed genes together with animals altered to carry the Cre gene that is downstream of a tissue or cell specific promoter. To visualise the expression of the floxed gene (or lack thereof), a fluorescent reporter gene is used. One such reporter gene is green fluorescent protein (GFP). The stop signal for the GFP gene is also flanked by two *LoxP* sites. In theory, expression of GFP indicates that gene knockout has been successful (101). To target the HPC region, it is possible to use the calcium/calmodulin-dependent protein kinase II alpha (CamKIIα) promoter, which is a promoter primarily active in HPC regions and other cortical regions (102). In addition, this is a promoter whose activity is low during embryonic development and early postnatal days, but the expression increases 10-fold in the frontal cortex by p16 (103). By p29, an adult pattern of recombination is established (102).

1.6 Aim

The main aim of this project was to elucidate whether TDG-mediated DNA demethylation is required for the hippocampal-dependent memory. We wanted to determine whether TDG depletion in the hippocampal areas has an impact on animal behaviour and memory. Three main objectives have been set for this to be achieved:

1) Determine where in the brain *Tdg* knockout occurs when using the conditional *Tdg* knockout mouse model CamKIIα-*Tdg*$^{-/-}$
2) Assess animal behaviour, LTM and STM of CamKIIα-*Tdg*$^{-/-}$ in various behaviour tasks
3) Optimizing the already established behavioural protocols used in our lab

2 Methodology

2.1 Ethics and animal housing

As this project utilises live animals, the principle of the three Rs (replacement, reduction, and refinement) was implemented to ensure efficient and humane animal research. All procedures involving animals were carried out in strict conformity with the Animal Welfare Act and the recommendations and laws established by the Norwegian Food Safety Authority. The FOTS application 24310 can be found at mattilsynet.no and provides more information regarding the food safety authority's ethical approval. The animals were housed at the Comparative Medicine Core Facility (CoMed) at St. Olav's Hospital in Trondheim. There they were provided with food (Ssniff V1536) and water *ad libitum*, and animal health was assessed daily. The cages were individually ventilated and located in the specific pathogen-free unit where humidity and temperature was set to 55-66% and 25° respectively, with a 12-hour reversed light-dark cycle.

2.2 Mouse model

The transgenic mouse model used in this study was CamKIIα-*Tdg*$^{-/-}$ (mini*Tdg*$^{+/+}$, Wt-*Tdg*$^{-/-}$ and CamKIIα-Cre$^{+/-}$). This transgenic strain has been generated by breeding female CamKIIα-Cre mice from Jackson laboratory (T29-1, stock #005359) (102) with male LoxP-mini*Tdg* (104). This transgenic strain was used as a *Tdg* knockout (KO) model, as this model contains a *LoxP* flanked mini*Tdg* (a thymine DNA-glycosylase mini gene), as well as a LoxP-STOP-LoxP cassette followed by an enhanced GFP (eGFP) sequence. In addition, this strain has a calcium/calmodulin-dependent protein kinase II alpha promoter (CaMKIIα) controlling Cre recombinase expression in hippocampal excitatory neurons at p29 (102). This enables conditional knockout of the *LoxP* flanked mini*Tdg* in adult animals (figure 3). The LoxP-mini*Tdg* strain was used as control group (mini*Tdg*$^{+/+}$, Wt-*Tdg*$^{-/-}$, and CamKIIα-Cre$^{-/-}$), as this model does not contain Cre recombinase to knock out mini*Tdg*.

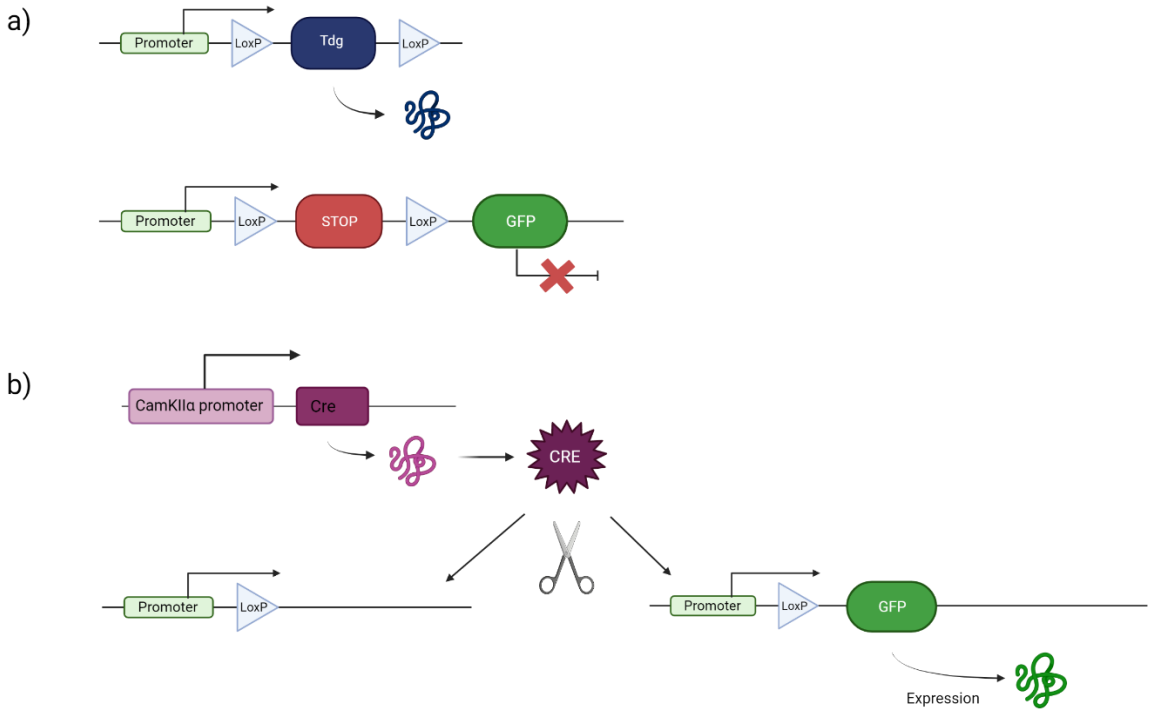

Figure 3. Excision of miniTdg and Stop signal by Cre recombinase in CamKIIα-Tdg$^{-/-}$ mice. a) The figure depicts the LoxP flanked genes of mini*Tdg* and the stop codon of GFP. As there is no active Cre recombinase, *Tdg* is expressed and GFP repressed. b) The figure depicts the CamKIIα promoter inducing expression of Cre recombinase, and this consequently leads to the removal of the mini*Tdg* gene and GFP stop signal. In turn, this leads to GFP expression and knockout of *Tdg*. The figure was created in Biorender.

2.3 Genotyping

The genotype of the animals was confirmed by polymerase chain reaction (PCR) and gel electrophoresis. Ear clippings were lysed in lysis buffer (10mM Tris, 1M KCl, 0.4% NP-40/Igpal CA360 Sigma, 0.1% Tween20) and protein kinase K (10mg/mL) before being incubated at 59°C overnight. The following day, the samples were heated to 95°C for 30 minutes, before being centrifuged (20 minutes, 14.000 rpm). The DNA from the supernatant was then diluted 1:10 in ddH_2O, before being added to a solution containing Taq 2x Master mix (10xPCR buffer, 2.5 mM dNTPs, 5U/µl paq5000, 50 mM $MgCl_2$), ddH_2O, and 0.5µM of each primer pair targeting the gene of interest (see table 1), making up a total volume of 10 µL.

The PCR programme was set to 95°C for 3 minutes, then 42 cycles of 95°C for 30 seconds, 64°C for 30 seconds, and 72°C for 1 minute. Lastly, there was an extension for 5 minutes at 75°C, followed by holding at 4°C indefinitely. The PCR products were separated by a 2% (w/v) agarose gel made with agarose (BioNordika LE Agarose), TAE buffer (Tris base, Glacial Acetic Acid, 0,5 EDTA), and 0,001% SybrSafe (Thermoficher/Invitrogen). PCR products together with 6X DNA loading dye (New England Biolabs), was loaded into the gel before it was run for 40 minutes at 120 V, and the results were visualised in UV exposure by the ChemiDocäMP imaging system (BIORAD). The size of the PCR products was determined by a 100bp DNA ladder.

Table 1. Primer sequences for PCR reactions

Allele	Primer	Sequence	Product size
mini*Tdg*	Compl Forward	AAATACTCTGAGTCCAAACCGGG	0.65 kb
	Tdg C Reverse	TGGTGAATCCGATGCCGTACTTG	
CAG-gfp	CAG-St-eGFP-Forward	CTTCAGCCGCTACCCCGACCACA	0.5 kb
	CAG-St-eGFP-Reverse	ATCGCGCTTCTCGTTGGGGTCTTT	
***Tdg* WT**	GT Tdg D Forward	TTGCGTGGGAGTAACCGAGC	0.6 kb
	GT Tdg B Reverse	GATGCACTCGGGAGACTTACAG	
CamKIIα-Cre	JAX_10884_Forward	GTTCTCCGTTTGCACTCAGG	0.3 kb
	JAX_oIMR8990_Reverse	CAGGTTCTTGCGAACCTCAT	

2.4 DNA purification

DNA purification of crude lysis was performed by using the magnetic beads extraction method. In a KingFisher™ deep well (Cat. Nr: A36586), row B was filled with 200 µL lysis buffer (10mM Tris, 1M KCl, 0.4% NP-40/Igpal CA360 Sigma, 0.1% Tween20), row C with 400 µL isopropanol, row D and E with 80% ethanol, and row F with RNase free water. 100 µL of previous lysis samples (see section 2.3 genotyping) were loaded in each well in row B, together with 400 µL beads dilution (20 µL Naxtra™ Magnetic beads, Lybe Scientific, Cat. Nr: LSMB0200 and 380 µL isopropanol). Part 1 of the KingFisher Duo Prime instrument for DNA was run, followed by addition of 50 µL RNase mix (1:20 RNase plus 1:5 RDS buffer in nuclease free water) to wells in row F, and 10 min incubation at room temperature. Afterwards, the sample was transferred to row A, followed by a washing step. Then, 400 µL isopropanol was added and part 2 of the programme was executed. Lastly, the final volume was transferred to a DNA low bind tube.

2.5 Behaviour

Long-term and short-term spatial memory performance and behaviour mice was assessed. Prior to habituation and handling, male mice were accustomed to the reverse light dark cycle for a minimum om 7 days. Handling was performed by letting the mouse smell the handler's hand and then lifting each mouse by the root of its tail a few times for 2-3 minutes once a day for three consecutive days before the start of the experiment. This was done to make the mice accustomed to being handled by the experimenter and to avoid novelty induced stress. After using this handling method for three months, another handling method was implemented to further reduce the stress put upon the animals, as it has been shown that that picking up mice by the tail induces anxiety levels and aversion (105). The new method involved the use of red cage tunnels to lift the mice, instead of lifting them by the tail. Prior to the start of the tests, the mice were left in the dark procedure room for 30 minutes to become acclimated to the environment. Animal movement in all the tests were recorded using the video tracking system ANY-maze. Between each trial and test, all surfaces in the mazes were cleaned using lemon soap water to avoid olfactory cues.

2.5.1 Open field test (OFT)

A white square box with the measurements 50x50x30 (LxWxH, in cm) was used in the open field test, where anxiety and exploration levels were assessed. One of the maze walls had a proximal cue attached to it. Mice were released in the corner closest to the experimenter (release corner, RC), and were allowed free exploration for 10 minutes. Movement of mice were recorded, and ANY-maze was used to divide the maze space into 16 squares, which were categorised as either centre, side, or corner zones (figure 4a).

2.5.2 Novel Object Location (NOL)

By modifying previously published protocols (88) the novel object location (NOL) test was used to investigate long-term memory (LTM) and short-term memory (STM) related to spatial reference memory. The box used for open field (OF) was also used in the NOL test, with the same cue card attached to the maze walls. Two identical objects, approximately 10 cm tall, were placed 12.5 cm from the maze walls with a 25 cm distance between the objects (figure 4b). When habituating for the test, the mice were allowed to explore the maze for ten minutes three times, with a hiatus of 24 hours between each session. On test day (day four), one of the objects were reallocated diagonally across the other object (figure 4b). The novelty preference is assessed by exploration time for the novel and familiar object location. The ANY-maze software recorded the time the mice spent in interaction with the objects, where proximity around the object were used as markers for exploration. Test was ended after animals spent 30 sec with the two objects combined, or 10 minutes had passed. The experimental setup for STM follows the same protocol as for LTM, except for an inter-trial interval of 5 minutes instead of 24h.

2.5.3 Y-maze

Another test used to investigate spatial LTM and STM, was the Y-maze test (93). A Y-shaped box with the measurements 35x7x15 (LxWxH, in cm) was used, where two distal cues were placed on the walls outside the maze (figure 4c). Prior to the test day, the mice were allowed free exploration for five minutes for six days with a 24 hour inter trial interval, where the entry to one of the arms was blocked. On test day, the mice were allowed entry to the novel arm. After a review of our protocols, changes were to optimize the procedure. Free exploration was allowed for three days with a 24 hour inter trial interval, and an object was placed in both the left and right arm during habituation and testing, to encourage exploration and further help the mice discern between the left, right, and release arm (figure 4c). The experimental setup for STM follows the same protocol as for LTM, except for an inter-trial interval of 5 minutes instead of 24h. Entries to each zone and time spent in each zone was recorded.

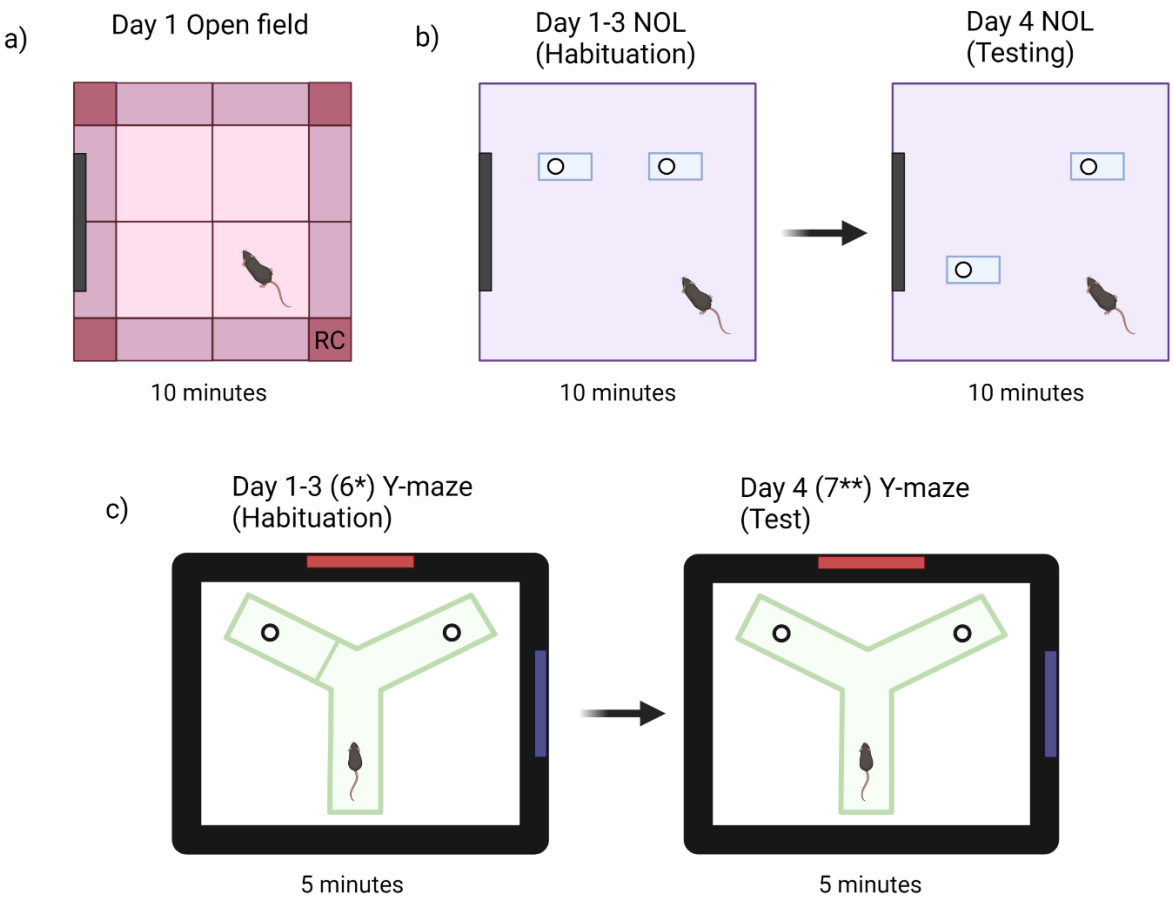

Figure 4. Behavioural paradigm setup used to test behaviour and spatial reference memory. a) The figure shows how the open field maze was divided into different zones: centre (light pink), sides (pink) and corners (dark pink). A black visual cue card is indicated on the left side of the wall. b) The figure shows the setup of objects during habituation and testing for NOL. A black visual cue card is indicated on the left side of the wall. c) The figure shows how the left arm area of the Y-maze is closed off during habituation and open during Y-maze test. The objects in the right and left arm were added to the setup after optimisation. Two different cue cards are placed on the walls of the arena. *Habituation lasted for six days pre optimization of protocol. ** test day was on day seven before optimization of the protocol. The figure was created using Biorender.

2.6 Perfusion

24h after the last behaviour test day, the mice were perfused with 0.9% saline and the brain was extracted for further analysis. The mice were put in an air-tight box with 1 mL isoflurane, then subsequently given a lethal intraperitoneal injection of pentobarbital (2mg/g), causing the animal to succumb to the overdose. Before continuing the procedure, paw pain reflexes were tested, and breathing was monitored to ensure that the right depth of anaesthesia had been reached. Next, the mouse was placed in a supine position, and a thoracic incision below the sternum was made, exposing the sternum. The ribcage was removed to get access to the heart. After clamping the ascending aorta, the right atrium was perforated, and the left ventricle was injected with approximately 60mL of 0.9% saline solution. After the procedure, the neck was severed, and the brain was collected for further

use by removing the cervical tissue and cranium bones. A sagittal cut was made dividing the brain in two halves, and these were either stored whole in 4% paraformaldehyde (PFA), or hippocampal microdissection was performed and collected for analysis.

2.7 Frozen sectioning

Extracted brains were stored in 4% PFA for a minimum of 48h before frozen sectioning. Frozen sectioning was performed using the Cryostar NX70 from Thermo Scientific. Both the objective and chamber temperatures were set to -20°C. To accelerate the freezing of the brain, the tissue was sprayed with freezing aerosol spray (PRF 101/520 ML GREEN NFL), then subsequently frozen by the cryogenic function of the machine. Lateral and medial sections were cut into 30µm and stored temporarily in 1x PBS with 0.03% ProClin™ 300 (Cat. No 48912-U) at 4°C. For long term storage, the sections were placed into freezing tubes with anti-freeze solution (40% PBS, 30% glycerol, 30% ethylene glycol) at - 20° C.

2.8 Immunohistochemistry

To determine if GFP expression and presumable *Tdg* knockout had occurred in CA1, CA3 and DG of the hippocampus, immunohistochemistry was performed on the tissue obtained from CamKIIα-*Tdg*$^{-/-}$ (knockout) and LoxP-mini*Tdg* (control) mice. 30µm brain sections (lateral and medial) from each mouse were incubated in 40 mM sodium citrate (Trisodium citrate 5,5 hydrate, Merk-Millipore 1.06431.1000) at 99°C for three minutes, to increase the detectability of antigens as the tissue previously had been fixed in PFA. The sections were retained in this solution until it had reached room temperature, for then to be washed 3x5 minutes in 1x PBS. To minimise unspecific antibody binding, the sections were incubated in blocking buffer (5% NGS/5% BSA/0,1% Triton X-100 in PBS) on a shaker (15 oscillations/min) for two hours at room temperature. Afterwards, the sections were incubated in dilution buffer (1% NGS/1% BSA/0,1%Triton X-100 in PBS) containing the primary antibodies (table 2) overnight in 4°C, at 15 oscillations/min. The next day, the sections were washed in PBS-T (1x PBS + 0,1% Tween20) three times, for 10, 20 and 30 minutes. Secondary antibodies (table 3) were diluted in the dilution buffer (1% NGS/1% BSA/0,1%Triton X-100 in PBS), before the slices were incubated in the secondary antibody solution in a light-protected container for two hours at room temperature on a shaker (15 oscillations/minute). After the incubation, the previous washing step was repeated. Lastly, the brain sections were mounted and stained with 1µg/mL DAPI in 1x PBS for one minute, then washed in 1x PBS twice and ddH_2O once before the slides were cover-slipped using mounting oil (ProLong™ Gold antifade reagent with DAPI, Invitrogen, Cat. No P36935). The slides were left in a light-protected container to dry overnight.

Table 2. Primary antibodies

Primary antibody	Isotype	Dilution	Manufacturer	Function
NeuN	mIgG1	1:500	Millipore, *Cat. Nr.* MAB377	Neuron nucleic marker. Staining of mature neurons.
GFP	rIgG mIgG1 mIgG2a	1:1000 1:500 1:1500	Invitrogen, *Cat. Nr.* A-11122 Thermo Fisher, *Cat. Nr.* MA5-15256 Thermo Fisher, *Cat. Nr.* A-11120	Gene reporter. Shows successful Cre activation and presumable Tdg depletion.

Table 3. Secondary antibodies

Secondary antibody	Isotype	Dilution	Manufacturer
A488	mIgG2a mIgG1 rIgG	1:1000	Invitrogen, *Cat. Nr.* A-21131 *Cat. Nr.* A-21121 *Cat. Nr.* A-11008
A555	rIgG mIgG1	1:1000	Invitrogen, *Cat. Nr.* A-21431 Thermo Fisher, *Cat. Nr.* A-21127

2.9 Fluorescence imaging using Zeiss confocal microscopy and Axioscan

To observe the fluorescence of the antibodies added to the brain slices during immunohistochemistry, stained sections were imaged with confocal laser scanning microscope Zeiss® LSM 880, together with the *Zen* software. GFP expression a in the hippocampal regions were investigated by applying a Plan-Apochromat 40X/NA oil immersion objective. The settings for pinhole, gain, and intensity were the same in each experiment, and were chosen depending on the excitation and absorbance from the fluorescent antibodies (NeuN and GFP). Z stack height was adjusted depending on each sample, by using the channel for neuronal marker NeuN to determine where the end and start of the slice depth was. The sections were also imaged using the high-performance slide scanner Zeiss® Axioscan Z1 with its corresponding zen software. This was to visualize

where GFP expression had occurred in the tissue using a 20x/0.8 M27 Plan Apochromat objective. Using a LED-Module 365nm light source, the signal from Dapi staining (A405 blue) was utilized to establish the correct focus. Light source intensity was adjusted according to what provided the best focus, which was 20,9% light source intensity with 20 ms exposure time. The GFP channel (A488 green) applied a LED-Module 470nm light source, and light source intensity was set to 40,0% where the exposure time was set to 30 ms, while the NeuN channel (A647 magenta) applied a LED-Module 625nm light source set to 30,0% intensity and 75 ms exposure time. Hippocampal GFP expression were analysed in the CA1, CA3 and DG areas of the hippocampus using IMARIS.

2.10 Image analysis

IMARIS Surfaces (Version 9.3.0, Oxford instruments) was used to visualise and investigate the GFP and NeuN expression in Hippocampal areas. GPF positive cells and NeuN positive cells were determined by manually creating a surface of the region of interest, and creating distinguished masked channels to discern where the IMARIS cell counting function would take place. The surface volume was the same in the masked channel of GFP and the masked channel of NeuN. The IMARIS function "spots" were used to count GFP and NeuN positive cells, where the cell size was set to 5 µm. Various detection thresholds were determined to calculate the number of spots for the different areas: 1.5 times mean intensity of the surface for the target channel when looking at GFP positive cells in CA1, and 2 times mean intensity of the surface for the areas of CA3 and DG. For NeuN positive cells, 1 times mean intensity of the surface for the target channel was used in all three areas. After selecting the thresholds, the number of spots were then given by the programme. As the volume of the surfaces was the same for the GFP masked channel and the NeuN masked channels, the percentage of GFP positive cells were given by dividing the number of GFP positive cells by the number of NeuN positive cells, then multiply by 100.

2.11 Statistical analysis

Data collected from OF, NOL and Y-maze were analysed in GraphPad Prism (version 9.4.1). Animals were grouped into LoxP-mini*Tdg* (control) and CamKIIα-*Tdg*$^{-/-}$ (Tdg-KO), 18m old LoxP-mini*Tdg*, and 4m old LoxP-mini*Tdg* mice. Outliers were identified in all instances by performing a ROUT test, and a Shapiro-Wilk test was performed to determine if the data was normally distributed. To determine if the test results were significantly above chance level (15 sec or 50%), a non-parametric one-sample t-test was performed. To determine if the results significantly differed between groups, an independent samples t-test or one-way ANOVA and post-hoc Tukey's HSD tests was performed. The statistical significance was set to a probability level of 95%.

3 Results

3.1 Verifying genotype by PCR and gel-electrophoresis

Previously in our lab, a neuron-specific *Tdg* knockout (KO) mouse model (CamKIIα-*Tdg*$^{-/-}$) was generated by crossing LoxP-mini*Tdg* mice (mini*Tdg*$^{+/+}$, Wt-*Tdg*$^{-/-}$) with a Tg(CamKIIα-Cre)T29 mouse strain from the Jackson laboratory (102,104). The first crossing produced heterozygous offspring with the genetic information mini*Tdg*$^{+/-}$, Wt *Tdg*$^{+/-}$ and CamKIIα-Cre$^{+/-}$. Female mice from the crossing (mini*Tdg*$^{+/-}$, Wt-*Tdg*$^{+/-}$ and CamKIIα-Cre$^{+/-}$) were further crossed with male LoxP-mini*Tdg* mice (mini*Tdg*$^{+/+}$, Wt-*Tdg*$^{-/-}$) to generate CamKIIα-*Tdg*$^{-/-}$ offspring with the genetic information mini*Tdg*$^{+/+}$, Wt-*Tdg*$^{-/-}$ and CamKIIα-Cre$^{+/-}$. Additionally, offspring with the genetic information mini*Tdg*$^{+/+}$ Wt-*Tdg*$^{-/-}$ and CamKIIα-Cre$^{-/-}$ were kept as control mice (LoxP-mini*Tdg*).

To further develop and maintain the newly generated mouse strain, I continued verifying the genotype of offspring from the heterozygous mating through PCR and gel electrophoresis. The primer pairs in table 1 were used to amplify the regions of the mini*Tdg* allele (size 650 base pairs, bp), Wt-*Tdg* allele (size 600 bp), eGFP allele (size 500 bp) and CamKIIα promoter (size 500 bp). In the CamKIIα-*Tdg*$^{-/-}$ mouse model (KO), we expect detection of PCR amplification of mini*Tdg*, eGFP, and CamKIIα. In the LoxP-mini*Tdg* mouse model (control), we expect to detect PCR amplification of mini*Tdg* and GFP. I set up new matings from the newly generated CamKIIα-*Tdg*$^{-/-}$ animals (mini*Tdg*$^{+/+}$, Wt-*Tdg*$^{-/-}$ and CamKIIα-Cre$^{+/-}$). A control strain was made by mating newly generated LoxP-mini*Tdg* female and male mice (mini*Tdg*$^{+/+}$, Wt-*Tdg*$^{-/-}$ and CamKIIα-Cre$^{-/-}$).

Surprisingly, we found wildtype (Wt) *Tdg* contamination from the offspring of new matings. This is exemplified in figure 5a, where offspring 1-3, 5 and 6 all had inherited the Wt-*Tdg* gene, while offspring 4 was confirmed to have the correct genetic information of the strains CamKIIα-*Tdg*$^{-/-}$ (mini*Tdg*$^{+/+}$, Wt-*Tdg*$^{-/-}$ and CamKIIα-Cre$^{+/-}$), and offspring 7 having the correct genotypes of LoxP-mini*Tdg* (mini*Tdg*$^{+/+}$, Wt-*Tdg*$^{-/-}$ and CamKIIα-Cre$^{-/-}$) control strain. Animals without the Wt-*Tdg* gene were selected to continue the breeding of the strains. The detection of Wt-*Tdg* indicated that the previous tests had been inadequate in detecting that allele. For troubleshooting, tests were repeated several times to exclude handling and contamination issues. On some re-runs, the PCR products indicating Wt-*Tdg* gene were detected by gel-electrophoresis, as shown in figure 5b, though not always. This indicates that the normal PCR using crude clipped ear sample lysate was not good enough to detect Wt-*Tdg*, and purification of DNA is necessary. Another reason could be that the resolution of the agarose gel used for gel-electrophoresis was not high enough to pick up the Wt-*Tdg* bands. Based on the unreliable Wt-*Tdg* results from genotyping, animals used previously in other experiments were re-tested to eliminate accidental Wt-*Tdg* positive animals. The re-testing included repeats of previous experiments, and purifying DNA from crude lysate by using the beads extraction method. In summary, more sensitive approaches need to be used when attempting to detect Wt-*Tdg* during PCR and gel-electrophoresis.

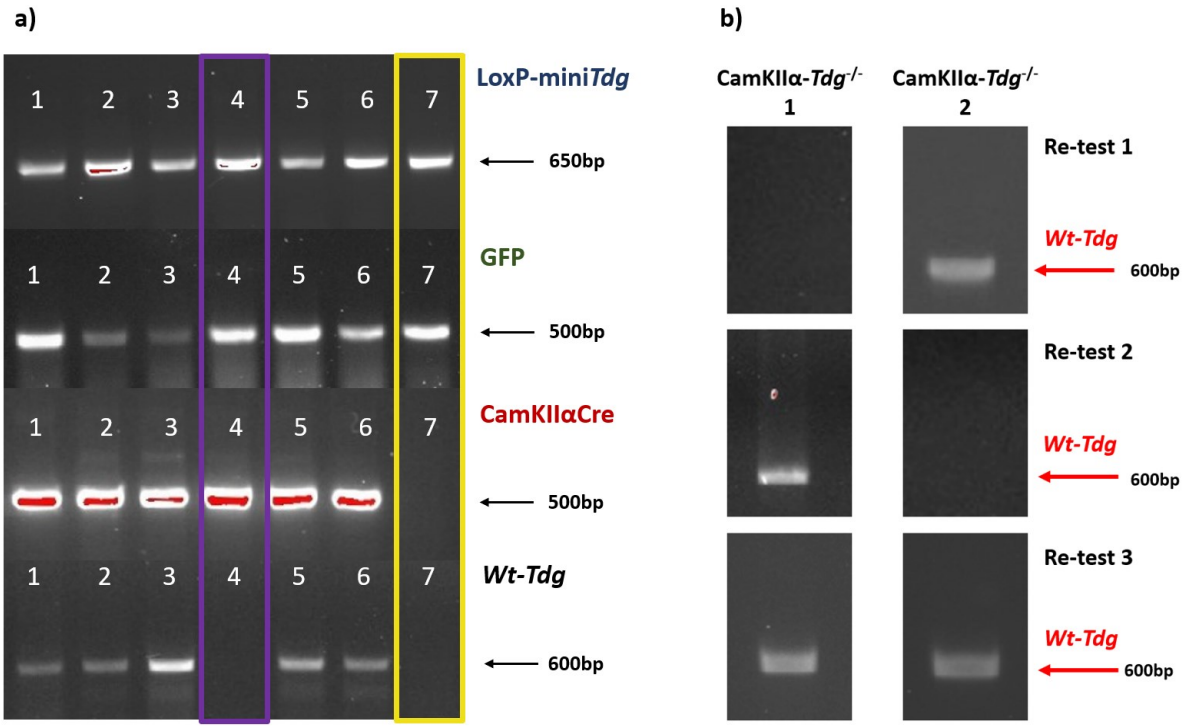

Figure 5. PCR and Gel-electrophoresis confirming genotype of animals. a) The image shows a selection of PCR results of offspring from new matings. The size of the PCR products (500-650 bp) is indicated alongside. The animal #4 with correct genotyping of CamKIIα-*Tdg*$^{-/-}$ strain is highlighted by the purple frame. The animal #7 with correct genotyping of is highlighted by the yellow frame. b) The images depict a selection of PCR results from two animals which were initially detected as Wt-*Tdg* negative but appeared to be positive when tested again. The size of the PCR products (600 bp) is indicated alongside.

3.2 Assessing Cre-induced GFP expression in the hippocampal region of CamKIIα-*Tdg*$^{-/-}$ mice

The CamKIIα-*Tdg*$^{-/-}$ mouse model induces neuron specific *Tdg* knockout. As the characterisation of the CamKIIα-Cre mouse strain, the CamKIIα promoter controls gene expression in excitatory neurons, primarily in the pyramidal layer of CA1 in the hippocampus (106). An adult pattern of Cre/LoxP recombination is established by postnatal day 29 (p29) (102). As illustrated in figure 3, the introduction of Cre-recombinase causes excision of the mini*Tdg* gene, as well as the GFP stop codon. Therefore, expression of GFP is indicative of Cre activity, and presumable *Tdg* knockout. Sagittal brain sections of CamKIIα-*Tdg*$^{-/-}$ mice were stained with antibodies against GFP and neuronal nuclear antigen (NeuN), and antibody expression was assessed using Axioscan and confocal imaging. GFP expression was expected predominantly in the CA1, as this is where the promoter is reportedly active. NeuN is used as a biomarker for mature neurons, enabling visualisation of adult neurons in the tissue. By a double-staining of GFP and NeuN antibodies, the efficiency of Cre-induced GFP expression in hippocampal neurons is assessed. As expected, NeuN-positive hippocampal neurons and GFP positive, presumably TDG-depleted neurons were detected in hippocampal subregions (figure 6).

The percentage of GFP positive neurons in hippocampal CA1, CA3, and DG of n = 6 CamKIIα-*Tdg*$^{-/-}$ was assessed and quantified using a 3D-image analysis software (IMARIS). The percentage of GFP positive neurons was determined by investigating how many of the

NeuN positive cells also were GFP positive. Figure 6e shows that around 80% of the neurons in CA1 were GFP positive (*M* = 85.3%, *SD* = 6.2). We expected most of the knockout to occur in this area due to the CamKIIα promotor primarily expressing Cre in CA1 of the HPC. We also observed that over 60% of the neurons in DG were GFP positive (*M* = 66.3%, *SD* = 10.7), suggesting substantial knockout in this area of the HPC as well. Figure 6e also shows that around 40-50% of the neurons in CA3 also expressed GFP (*M* = 45.5%, *SD* = 7.8). In summary, these results indicate that GFP expression is strongest in CA1, followed by DG and CA3. This suggest that Cre expression and *Tdg* knockout occurs in the HPC region, mostly in the CA1. This was as expected due to the expression pattern of the CamKIIα promotor.

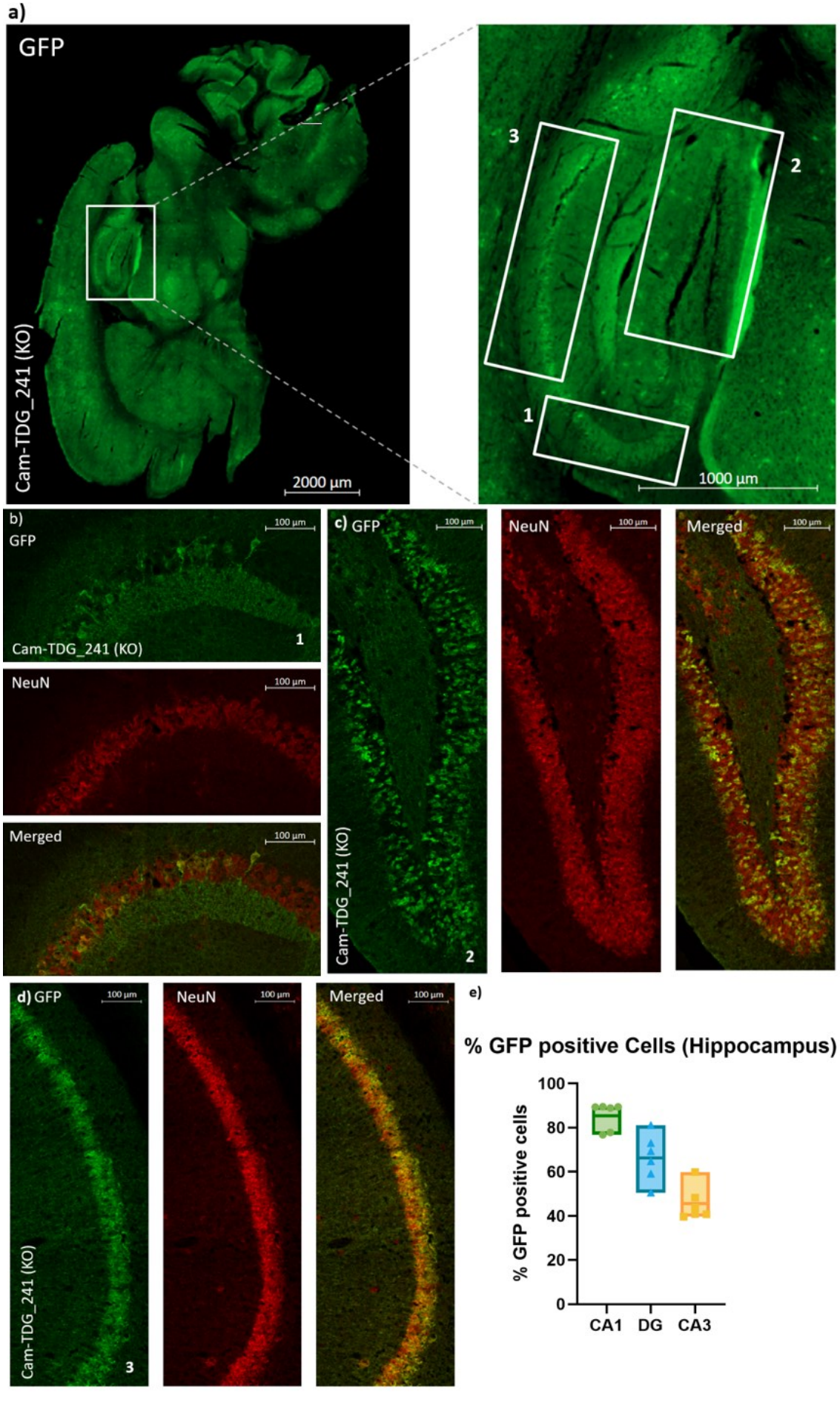
a)
GFP
Cam-TDG_241 (KO)
2000 µm
3
2
1
1000 µm
b)
GFP
100 µm
Cam-TDG_241 (KO)
1
NeuN
Merged
c) GFP
Cam-TDG_241 (KO)
2
d) GFP
Cam-TDG_241 (KO)
3
e)
% GFP positive Cells (Hippocampus)
% GFP positive cells
100
80
60
40
20
0
CA1
DG
CA3

Figure 6. Hippocampal GFP expression in CamKIIα-Tdg$^{-/-}$ mice brain tissue. a) Axioscan from Zeiss. The images show Cre-Induced GFP expression in a CamKIIα-*Tdg*$^{-/-}$ mouse (*Tdg*-KO), which is indicated by green fluorescence. Strong GFP expression is observed in HPC regions (1, 2, 3). b) The images show Cre-induced GFP expression and NeuN expression (red fluorescence) in CA3 in a 3-month-old CamKIIα-*Tdg*$^{-/-}$ mouse (confocal). c) The images show Cre-induced GFP expression and NeuN expression (red fluorescence) in DG in a CamKIIα-*Tdg*$^{-/-}$ mouse (confocal). d) The images show Cre-induced GFP expression and NeuN expression (red fluorescence) in CA1 in a CamKIIα-*Tdg*$^{-/-}$ mouse (confocal). e) The graph shows the calculated ratio of GFP positive cells in CA1, CA3, and DG of n = 6 CamKIIα-*Tdg*$^{-/-}$ mice. Coloured dots represent individual animals. Images were processed in Zen software (Zeiss). The graph was created in GraphPad Prism.

3.3 Assessing anxiety of CamKIIα-*Tdg*$^{-/-}$ mice

An open field test was used to assess anxiety levels in CamKIIα-*Tdg*$^{-/-}$ mice. High levels of stress and anxiety can impact performance in other behavioural tests, as mice with high levels of anxiety might be more averse to explore the environment (107). A total number of 45 mice were subjected to testing. Animals that did not complete the test, and animals contaminated with Wt-*Tdg* were excluded from the test. 22 3–4-month-old male LoxP-mini*Tdg* mice (control), 15 3–4-month-old male CamKIIα-*Tdg*$^{-/-}$ mice (*Tdg*-KO), and 7 LoxP-mini*Tdg* 18–19-month-old male mice. An overview of the groups can be seen in table 4. Normal distribution of included samples was investigated using a Shapiro-Wilk test. Removal of any outliers identified by a ROUT (Q = 1%) test has been performed. All dependent variables satisfy relevant statistical test assumptions. The mean (*M*) and standard deviation (*SD*) is given for all tests. The significance level α was set to .05 for the statistical tests.

Table 4. Overview over animals used in behaviour studies

Group of animals	Number of animals	Genotype	Name referred to in figures	Source of animals
CamKIIα-*Tdg*$^{-/-}$ mice male mice (3-4m)	15	mini*Tdg*$^{+/+}$, Wt-*Tdg*$^{-/-}$ and CamKIIα-Cre$^{+/-}$	*Tdg*-KO	Crossing LoxP-mini*Tdg* mice with Tg(CamKIIα-Cre)T29
LoxP-mini*Tdg* (3-4m)	18	mini*Tdg*$^{+/+}$ Wt-*Tdg*$^{-/-}$ and CamKIIα-Cre$^{-/-}$	Control	Crossing LoxP-mini*Tdg* mice with Tg(CamKIIα-Cre)T29
LoxP-mini*Tdg* (4m)	4	mini*Tdg*$^{+/+}$ Wt-*Tdg*$^{-/-}$ and CamKIIα-Cre$^{-/-}$	4-month-old *Tdg*-mice	Original LoxP-mini*Tdg* strain
LoxP-mini*Tdg* (18-19m)	7	mini*Tdg*$^{+/+}$ Wt-*Tdg*$^{-/-}$ and CamKIIα-Cre$^{-/-}$	18-19-month-old *Tdg*-mice	Original LoxP-mini*Tdg* strain

The exploration activity and anxiety levels of the animals were measured by investigating how long time they spent in the corners and centre. Animals spending more time in the open exposed centre of the maze are associated with being less anxious and exhibiting an increased exploratory behaviour, compared to mice spending more of their time in the corners (108). Data concerning time (sec) spent in the different regions of the maze was collected.

The CamKIIα-*Tdg*$^{-/-}$ mice (*Tdg*-KO) group (n = 15) spent less time in the centre (mean difference in time *M* = 141 sec, *SD* = 56) than in the corners (*M* = 197 sec, *SD* = 49). But the difference was not significant, paired t-test, , $t(14) = 2.10$, $p = .054$ (Figure 7). The LoxP-mini*Tdg* (control) group (n = 18) spent significantly more time in the corners (*M* = 194 sec, *SD* = 37) than in the centre (*M* = 136 sec, *SD* = 43.8), paired t-test $t(17) = 3.14$, $p = .006$. An independent samples t-test showed that there was no significant difference between the control and *Tdg*-KO groups in time (sec) spent in the corners, $t(31) = .18$, $p = .860$. The same was true for the amount of time (sec) spent in centre for both genotypes, $t(31) = .26.$, $p = .793$. To summarise, though both *Tdg*-KO and control group spent less time in the centre, the results indicate there was no significant difference in anxiety levels between the groups.

In addition, the aged LoxP-mini*Tdg* mice (18-19-monts old, *n* = 7), spent less time in the corner zones (*M* = 148 sec, *SD* = 35.9) than in the centre (*M* = 184 sec, *SD* = 42.2). However, the difference was not significant $t(6) = 1.40$, $p = .212$. In contrast, the young 4-month-old *Tdg*-mice (n = 4) spent similar time in the corners (*M* = 170 sec, SD = 24.7) as in the centre (*M* = 175 sec, SD = 28.8), paired t-test significant $t(3) = .21$, $p = .849$.

An independent samples t-test showed that there was no significant difference between the young and aged groups in time (sec) spent in the corners, $t(9) = .025$, $p = .332$, and in the centre, $t(9) = .57$, $p = .583$. In summary, neither young nor aged *Tdg*-KO mice showed elevated forms of anxiety.

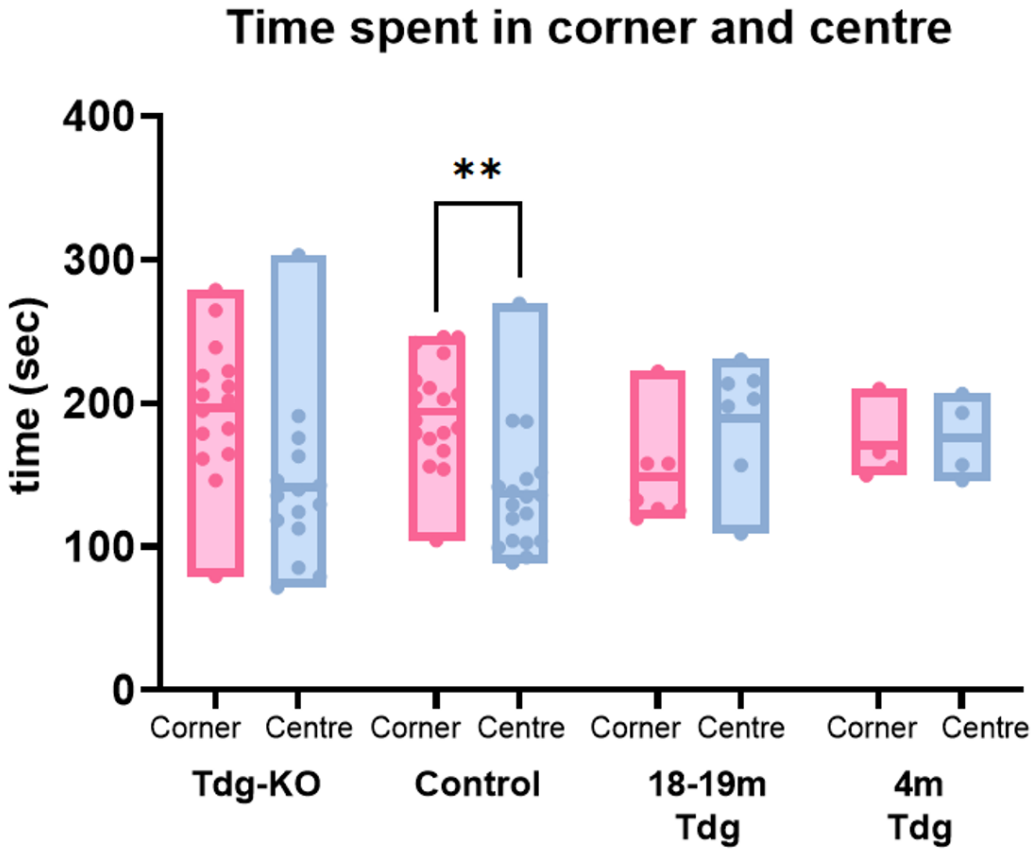

Figure 7. Boxplot visualising time spent in the corner and centre of the OF test maze for CamKIIα-Tdg$^{-/-}$ (Tdg-KO), Control, 18-19-month-old and 4-month-old Tdg-mice. Coloured dots represent individual animals. The graph shows performance for all animals: CamKIIα-*Tdg*$^{-/-}$ (n = 15), Control (n = 18), 18-19-month-old *Tdg* (n = 7), and 4-month-old *Tdg* mice (n = 4). ** = p < .01, paired t-test. Graph was created in GraphPad Prism.

3.4 Assessing long-term and short-term memory of CamKIIα-*Tdg*$^{-/-}$ mice by behavioural studies

DNA methylation is a key regulator of transcriptional regulation, and regulation of methylation patterns in the hippocampus is considered as an important component for the formation and storage of memory (35,55). Behavioural tests were used to determine if hippocampal *Tdg* depletion had any impact on spatial memory. Our group has established behavioural tasks, the novel object location (NOL) task and the Y-maze, to assess short-term and long-term memory components (88,93). Both tests exploit mice's inherent preference for a novel environment to assess spatial memory. A total number of 45 mice were subjected to testing. 22 3–4-month-old male LoxP-mini*Tdg* mice (control), 15 3–4-month-old male CamKIIα-*Tdg*$^{-/-}$ mice (*Tdg*-KO), and 7 LoxP-mini*Tdg* 18–19-month-old male mice. An overview of the groups can be seen in table 4. *Tdg*-KO and control animals were tested for long- and short-term spatial reference memory. For long term spatial memory, two different protocols were used: the already established behaviour protocol in

our lab, and an optimised protocol (described in methods section). Additionally, young (4m) and aged (18-19m) animals were tested for long term spatial memory using the optimised protocol, to ascertain that old age affects spatial memory, and to get familiarised using the new protocol. Animals that did not complete the test (e.g., not exploring any objects before 10 min passed in NOL, or animals climbing out of the maze etc.), and animals discovered to be Wt-*Tdg* positive, were excluded from the test. Normal distribution of included samples was investigated using a Shapiro-Wilk test. Removal of any outliers identified by a ROUT (Q = 1%) test has been performed. All dependent variables satisfy relevant statistical test assumptions. The mean (*M*) and standard deviation (*SD*) is given for all tests. The significance level α was set to .05 for the statistical tests.

3.4.1 Novel Object Location test

To assess spatial reference memory, the NOL task was performed. The preference for a spatial location, whether novel or familiar, was investigated by measuring the time the animals spent exploring the object locations. For the long-term memory (LTM) condition (24h inter-trial interval), we expect that mice with normal spatial long-term memory would spend relatively more time in the novel object zone than mice with impaired long-term spatial memory. Normal mice have an inherent curiosity and preference for novel location (109). Animals with impairment in spatial reference memory will not be able to recognise the novel object location, and therefore alternate as if both object locations were novel. Animals with impaired working memory (STM) are expected to alternate when using the short-term memory (STM) condition (5 min inter-trial interval). The time spent in each location was also compared to a defined chance level (15 sec), as a measure of preference for a novel environmental aspect. If the test fulfils the requirements of a spatial memory test, we expect the control group to show a clear preference for NOL. 32 mice were tested in the LTM condition, and 14 mice in the STM condition. The test was stopped after the animals had spent a combined of 30 seconds exploring the objects, or after 10 minutes had passed if the exploration activity was below 30 seconds, seen as a non-fulfilment of the test. A one sample t-test was used to determine if the animals spent significantly more time in NOL than chance level. An independent samples t-test was used to determine significant difference between groups.

3.4.1.1 Long term memory

The control group (n = 11) spent significantly more time (sec), above chance level (15 sec), in NOL (M = 19.7 sec, SD = 4.2) one sample t-test $t(10) = 3.65$, $p = .004$ (figure 8a), suggesting that the control mice have normal long-term spatial memory as expected. The *Tdg*-KO group (n = 8) spent less time in NOL compared to the control group, but still show weak significance above the 15-sec chance level (M = 17.4 sec, SD = 2.1), one sample t-test $t(7) = 3.28$, $p = .013$ (figure 8a). So far, no statistical significant difference was detected between the control and *Tdg*-KO groups (independent samples t-test, $t(17) = 1.35$, $p = .194$), which may be due to the small sample size. In summary, these results suggest that the CamKIIα-$Tdg^{-/-}$ mice may exhibit impaired long-term spatial memory in the NOL task, but more animals need to be included in the test to show the statistical difference.

3.4.1.2 Short term memory

The control group (n = 7) spent more time (sec) in NOL than in familiar location (M = 16.84, SD = 4.59), though unexpectedly, this preference was not significantly above the 15-sec chance level (15 sec), one sample t-test $t(6) = 1.06$, $p = 329$ (figure 8b), which may be due to the small sample size. Likewise, the *Tdg*-KO group (n = 7) spent more time

in NOL, though not significantly above chance level (M = 16.3, SD = 5.7), one sample t-test $t(6) = .60$, $p = .572$ (figure 8b). Further, no statistical significant difference was detected between the control and *Tdg* groups (independent samples t-test, $t(12) = .20$, $p = .844$. In summary, these results suggest that the CamKIIα-*Tdg*$^{-/-}$ mice may exhibit impaired short-term memory in the NOL task, but more animals need to be included in the test to show the statistical difference.

3.4.1.3 Long term memory in aged animals

Knowing that older animals show spatial memory impairment (110), we used aged and young LoxP-mini*Tdg* mice to assess our newly optimised protocol. The young LoxP-mini*Tdg* mice (4-moths old, $n = 4$) spent more time, above chance level (15 sec) in NOL (M = 21.9, SD = 1.6), one sample t-test $t(3) = 8.38$, $p = .004$ (figure 8c), suggesting that the young animals have normal long-term spatial memory as expected. The aged LoxP-mini*Tdg* mice (18-19-monts olds, $n = 7$) spent marginally less time in NOL compared to the young mice, but still show strong significance above the 15 sec chance level (M = 21 sec, SD = 1.5), one sample t-test $t(6) = 10.34$, $p < .0001$ (figure 8c). No statistical significance was detected between the young and aged LoxP-mini*Tdg* group (independent samples t-test, $t(9) = .83$, $p = .426$. In summary, the results suggest that the aged LoxP-mini*Tdg* mice do not exhibit impaired long-term spatial memory, but more animals need to be included in the test to show the statistical difference.

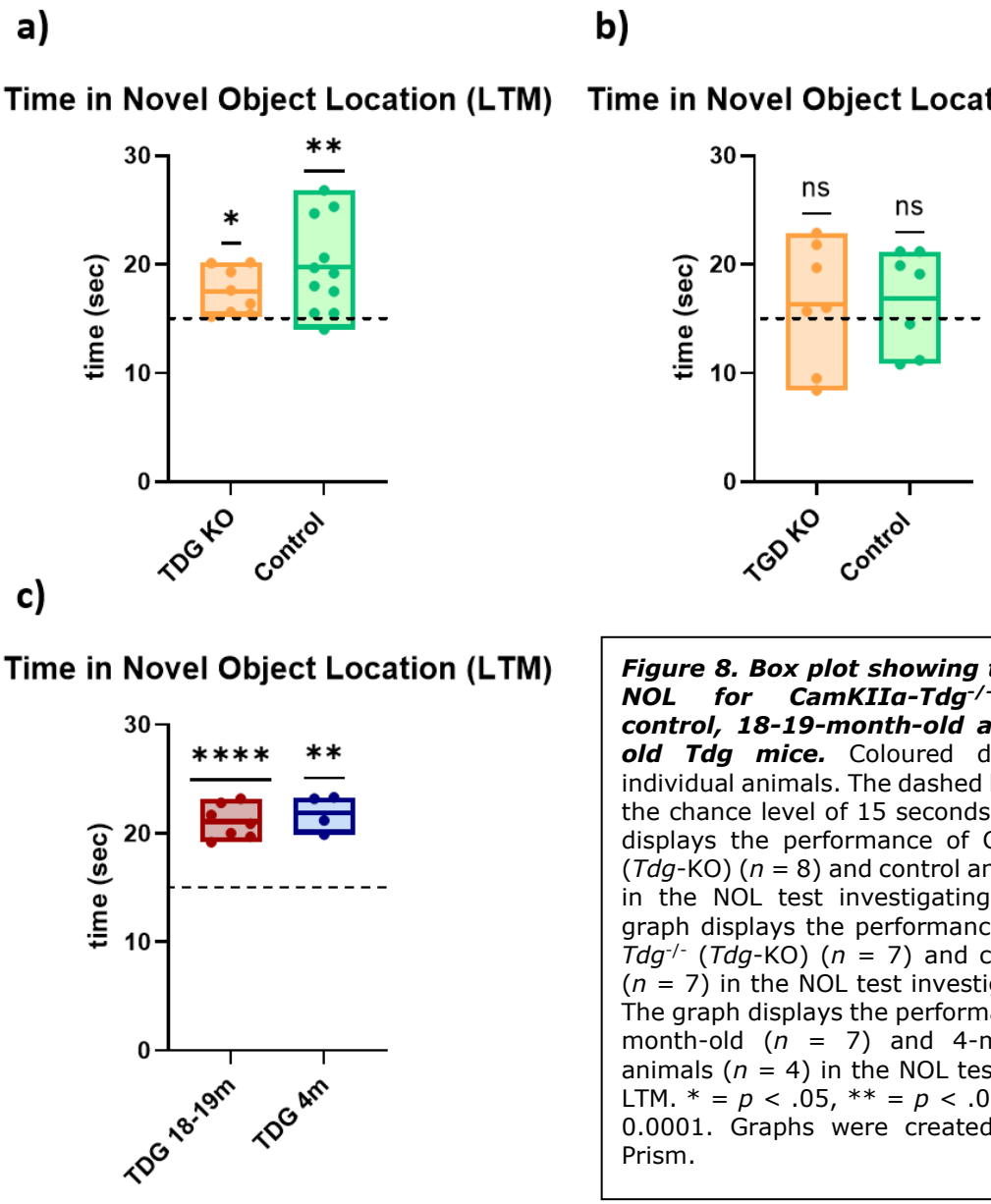

Figure 8. Box plot showing time spent in NOL for CamKIIα-Tdg$^{-/-}$ (Tdg-KO), control, 18-19-month-old and 4-month-old Tdg mice. Coloured dots represent individual animals. The dashed lines represent the chance level of 15 seconds. a) The graph displays the performance of CamKIIα-*Tdg*$^{-/-}$ (*Tdg*-KO) (n = 8) and control animals (n = 11) in the NOL test investigating LTM. b) The graph displays the performance of CamKIIα-*Tdg*$^{-/-}$ (*Tdg*-KO) (n = 7) and control animals (n = 7) in the NOL test investigating STM. c) The graph displays the performance of 18-19-month-old (n = 7) and 4-month-old *Tdg* animals (n = 4) in the NOL test investigating LTM. * = p < .05, ** = p < .01, **** = p < 0.0001. Graphs were created in GraphPad Prism.

3.4.2 Y-maze test

The Y-maze test was performed to further investigate behaviour indicating potential performance differences in spatial memory of the groups The test is used to assess spatial reference memory by determining if animals have a preference to a novel environment, or just alternate randomly between a novel and familiar environment. An animal with normal spatial reference memory was expected to spend more time in the novel location than in the familiar. The percentage of entries to, and the percentage of time spent in the novel environment was compared to a defined chance level (50%), as a measure of preference for a novel environment. If the test fulfils the requirements of a spatial memory test, we expect the control group to show a clear preference for the novel arm. In addition, the total amount of entries to, and total amount of time spent in the three different Y-maze arms was investigated. 14 mice were tested in the long-term condition (24h inter-trial

interval) using the old protocol, 17 mice were tested in the long-term condition using the optimized protocol, and 11 mice were tested in the short-term condition using the optimised protocol (5 min inter-trial interval). As a reminder, the optimised protocol included identical objects in the novel and familiar right arm and a decreased amount of habituation periods in the test.

3.4.2.1 Total number of entries to each of the arms in the Y-maze

Observations of total number of entries to each of the arms were performed to determine the exploration interest of the mice before and after protocol optimisation. We wanted to investigate if the previously described measures we had implemented increased the animals interest to explore more in the novel and familiar right arm, as these are the variables used when determining novelty preference using the Y-maze protocol in our lab. This is because when the animals are released in the familiar release arm, they get the option to choose between the novel and familiar right arm.

Long term condition (old protocol)

The LoxP-mini*Tdg* (control) group (n =7) had significant differences in entries to the Y-maze arms, one-way ANOVA $F(2, 18) = 7.89$, $p = .004$. A post hoc Tukey test was performed to examine pairwise differences among the familiar right (M = 8.4, SD = 1.8), familiar release (M = 14.5, SD = 3.5), and novel arm (M = 17.1, SD = 6.1) Results revealed that the control group had less entries to the familiar right arm than to both the novel, $p = .003$, and familiar release arm, $p = .035$, but the difference in entries to the novel arm and familiar release arm was not significant, $p = .503$ (figure 9a). The CamKIIα-*Tdg*$^{-/-}$ (*Tdg*-KO) group (n = 7) had significant differences in entries to the Y-maze arms, one-way ANOVA $F(2, 18) = 5.24$, $p = .016$. A post hoc Tukey test was performed to examine pairwise differences among the familiar release (M = 14, SD = 4.5), the novel (M = 15, SD = 4.3) and the familiar right arm (M = 8.3, SD = 3.7) (figure 9a). The results revealed that the *Tdg*-KO mice had a significantly lower number of entries to the familiar right arm than to the novel, $p = .020$, and familiar release arm, $p = .050$, while the difference in entries to the novel arm and familiar release arm was not significant, $p = .896$. In summary, the results suggest that both control and *Tdg*-KO groups are less interested in exploring the familiar right arm before protocol optimisation, though more animals need to be added to increase the statistical power.

Long term condition (new protocol)

The control group (n = 4) had fewer entries to the familiar release arm (M = 9.5, SD =2.8) than to the novel (M = 13.7, SD = 3.6) and familiar right (M = 11.7, SD = 4.2), though no differences in entries were statistically significant, one-way ANOVA $F(2, 9) = 1,35$, $p = .307$ (figure 9b). The *Tdg*-KO group (n = 2) had fewer entries to the release arm (M = 10.5, SD = 0.7) than to the novel (M = 18.5, SD = 7.7) and familiar right arm (M = 14, SD = 4.2), but no differences in entries were statistically significant, one-way ANOVA, $F(2, 9) = 1,35$, $p = .307$ (figure 9b). In summary, the results suggest that both control and *Tdg*-KO groups are less interested in exploring the familiar release arm after protocol optimisation, but we need more animals to show statistical difference.

Short term condition (new protocol)

The control group (n = 4) had fewer entries to the familiar right arm compared to the others, but had no significant difference in entries between the novel (M = 11.2, SD = 6.0), familiar right (M = 4.2, SD = 2.7) and familiar release arm (M = 10.0, SD = 7.0), one-way ANOVA, $F(2, 9) = 1.74$, p = .229 (figure 9c), which may be due to the small sample size. The *Tdg*-KO mice (n = 7) had significant differences in entries to the Y-maze arms, one-way ANOVA $F(2, 18) = 8.02$, p = .003. A post hoc Tukey test was performed to examine pairwise differences between the familiar release (M = 23, SD =14.9), the novel (M = 9.5, SD = 3) and the familiar right arm (M = 4.8, SD = 1.2) (figure 9c). Results revealed that the *Tdg*-KO mice had a significantly higher number of entries to the familiar release arm than to the novel, p = .026, and familiar right arm, p = .003. The difference in entries to the novel arm and the familiar release arm was not significant, p = .507. In summary, the results suggest the *Tdg*-KO group was surprisingly interested in exploring the familiar release arm, and the control animals were less interested in exploring the familiar right arm after protocol optimisation indicating that the optimisation did not work, though more animals are needed to show statistical difference.

Long term condition testing young and aged mice (new protocol)

The young (4-moth-old) LoxP-mini*Tdg* group (n = 4) had fewer entries to the familiar right arm compared to the others, but had no significant difference in entries between the novel (M = 14.5, SD = 5.6), familiar right (M = 10.7, SD = 3.4) and the familiar release arm (M = 14.7, SD = 3.6), one way ANOVA $F(2, 9) = 1.05$, p = .390 (figure 9d). The aged (18-19-moth-old) LoxP-mini*Tdg* group (n = 7) had no significant difference in entries to the novel (M = 10.5, SD = 3.8), familiar right (M = 10.5, SD = 4.3), and familiar release arm (M = 10.4, SD = 2.9), one-way ANOVA $F(2, 18) = .003$, p = .997 (figure 9a). In summary, the results suggest that the young mice were less interested in exploring the familiar right arm, while the aged were equally interested in exploring each arm when using the optimised protocol. However, more animals are needed to show statistical difference.

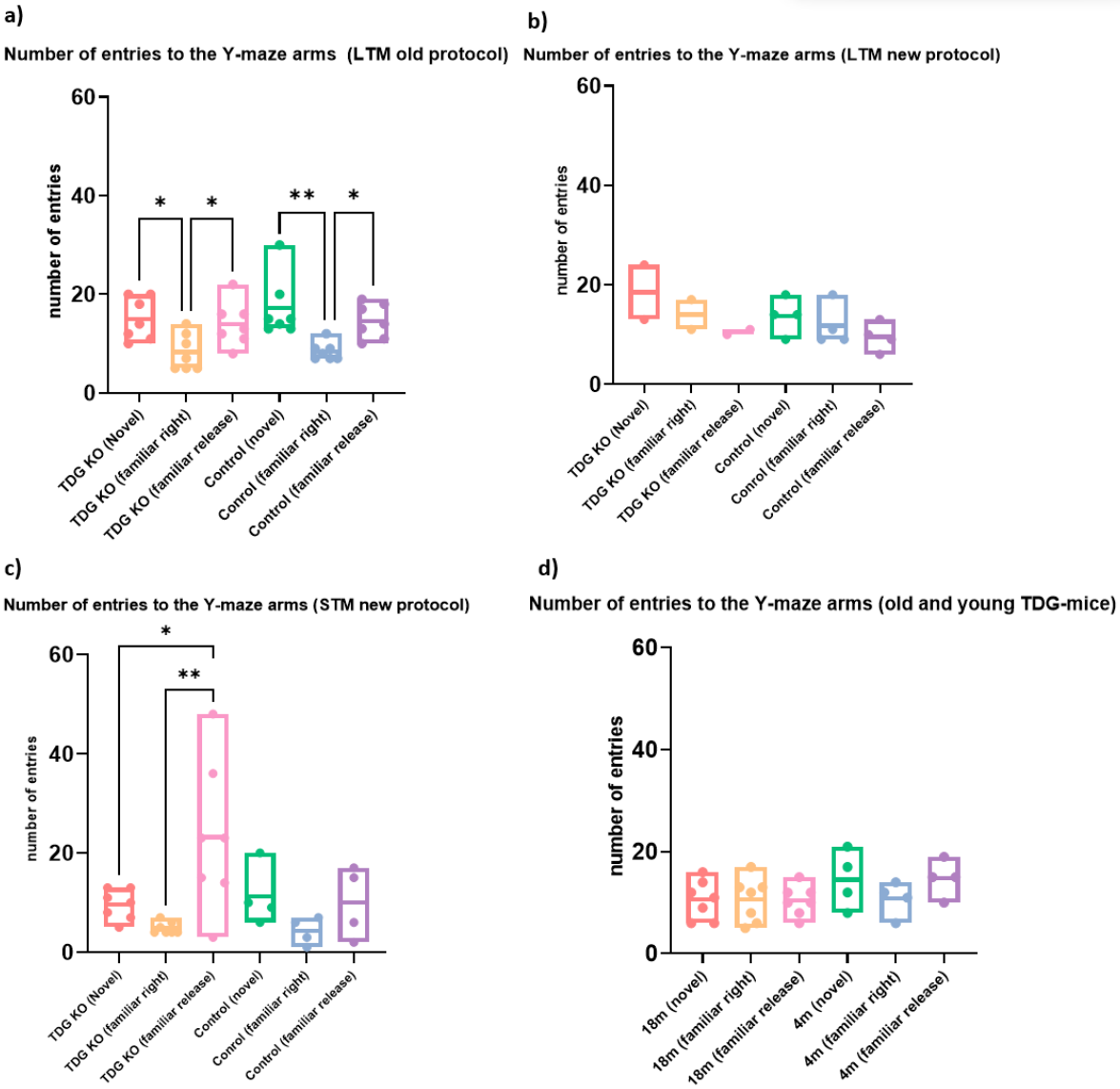

Figure 9. Total number of entries to novel left, familiar right, and familiar release arm in the Y-maze test. Individual mice are represented by coloured dots. Statistically significant difference between groups is determined by one-way ANOVA and post-hoc Tukey's HSD test. a) The graph shows number of entries to the Y-maze arms by CamKIIα-*Tdg*$^{-/-}$ (*Tdg*-KO) (n = 7) and control mice (n = 7) when testing long term spatial memory using the old established protocol. b) The graph shows number of entries to the Y-maze arms by CamKIIα-*Tdg*$^{-/-}$ (Tdg-*KO*) (n = 2) and control mice (n = 4) when testing long term spatial memory using the optimised protocol. c) The graph shows number of entries to the Y-maze arms by CamKIIα-*Tdg*$^{-/-}$ (*Tdg*-KO) (n = 7) and control mice (n = 4) when testing short term spatial memory using the optimised protocol. d) The graph shows number of entries to the Y-maze arms by 18-19-month-old (n = 7) and 4-month-old (n = 4) *Tdg* mice when testing long term spatial memory using the optimised protocol. * = p < .05, ** = p < 0.01. The graphs were created in GraphPad Prism.

3.4.2.2 Total amount of time spent in the three Y-maze arms

Observations of total the total amount of time (sec) spent in each of the arms were performed to determine the exploration interest of the mice before and after protocol optimisation. We wanted to investigate if the previously described measured we had implemented increased the animals' interest to explore more in the novel and familiar right arm, as these are the variables used when determining novelty preference using the Y-

maze protocol in our lab. This is because when the animals are released in the familiar release arm, they get the option to choose between the novel and familiar right arm.

Long term conditions (old protocol)

The control group (n = 7) had significant differences in time (sec) spent in Y-maze arms, one-way ANOVA $F(2, 18) = 15.57$, $p = .0001$. A post hoc Tukey test was performed to examine pairwise differences among the familiar release (M = 36.1 seconds, SD = 9.2), the novel (M = 92 seconds, SD = 9.2), and the familiar right arm (M = 80.3 seconds, SD = 29.1). The results revealed that the control group spent less time in familiar release arm than in both the novel, $p = .0001$, and familiar right arm, $p = .002$ (figure 10a). The difference in time spent in the novel and familiar right arm was non-significant, $p = .524$. The *Tdg*-KO group (n = 7) had significant differences in time (sec) spent in Y-maze arms, one-way ANOVA $F(2, 18) = 9.16$, $p = 0.002$. A post hoc Tukey test was performed to examine pairwise differences among the familiar release (M = 41.3 sec, SD = 17.4), novel (M = 90.5 sec, SD = 21.4) and familiar right arm (M = 68.2 sec, SD = 25.2). The results revealed that the *Tdg*-KO group spent significantly more time in the novel arm than in the familiar release arm, $p = .002$. The difference in time spent in the novel and familiar right arm was non-significant, $p = .159$, as well for the difference between the familiar right and familiar release arm, $p = .076$ (figure 10a). In summary, the results suggest that both the control and *Tdg*-KO groups were less interested in exploring the familiar release arm when using the old protocol, but the addition of more animals are needed to increase the statistical power.

Long term conditions (new protocol)

The control group (n = 4) spent less time (sec) in the familiar release arm (M = 46.6 sec, SD = 15.5) than in novel (M = 74 sec, SD = 12.5) and familiar right arm (M = 78.2 sec, SD = 28.4), but no differences in amount of time were statistically significant, one-way ANOVA $F(2, 9) = 2.92$, $p = .105$ (figure 10b). The *Tdg*-KO group (n = 2) had significant differences in time in the Y-maze arms, one-way ANOVA $F(2, 3) = 29.15$, $p = .011$. A post hoc Tukey test was performed to examine pairwise differences among the familiar release (M = 38.6 sec, SD = 0.5)., the (M = 88.6 sec, SD = 0.3) and the familiar right arm (M = 101.9 sec, SD = 15). The results revealed that the *Tdg*-KO group spent less time in the familiar release arm than the novel, $p = .022$, and familiar right arm, $p = .011$ (figure 10b). The difference in time spent in the novel arm compared to the familiar right arm was non-significant, $p = .401$. In summary, the results suggest that both the control and *Tdg*-KO group were less interested in exploring the familiar release arm, but more animals need to be included in the test to show the statistical difference.

Short term conditions (new protocol)

The control group (n = 4) spent less time in the familiar right arm (M = 30.4 sec, SD = 16.2) than in the novel (M = 77.8 sec, SD = 22.1) and familiar release arm (M = 95.7 sec, SD = 83.5), but no differences in amount of time were statistically significant, one-way ANOVA $F(2, 9) = 1,76$, $p = .226$ (figure 10c). The *Tdg*-KO group (n = 7) had significant differences in time (sec) spent in Y-maze arms, one-way ANOVA $F(2, 18) = 7.35$, $p = .016$ (figure 10c). A post hoc Tukey test was performed to examine pairwise differences among the novel ((M = 100.7 sec, SD = 35.4), familiar right (M = 49.5 sec, SD = 17.5), and familiar release arm (M = 55.2 sec, SD = 26.4). The results revealed that the *Tdg*-KO group spent more time

in the novel arm compared to the familiar right, p = .007, and familiar release arm (p = .016). The difference in time spent in the novel arm compared to the familiar right arm was not significant, p = .921. In summary, results suggest that the control group was less interested in exploring the familiar right arm, while the *Tdg*-KO group was more interested in exploring the novel arm, but more animals need to be included in the test to show the statistical difference.

Long term condition testing young and aged mice (new protocol)

The young LoxP-mini*Tdg* group (n = 4) had significant differences in time (sec) spent in Y-maze arms, one-way ANOVA $F(2, 9) = 9.52$, p = .006. A post hoc Tukey test was performed to examine pairwise differences among the familiar release (M = 27.8 sec, SD = 11.2), novel (M = 102.8 sec, SD = 25.3) and the familiar right arm (M = 83.8 sec, SD = 33.8). The results revealed that the young group spent significantly less time in the familiar release than in both the novel, p = .006, and familiar right arm, p = .029 (figure 10d). The difference in time spent in the novel and familiar right arm was not significant, p = .560. The aged LoxP-mini*Tdg* group (n = 7) had significant differences in time (sec) spent in Y-maze arms, one-way ANOVA $F(2, 15) = 35.67$, $p < .0001$. A post hoc Tukey test was performed to examine pairwise differences among the familiar release (M = 40.8 sec, SD = 9.4), novel (M = 85.2 sec, SD = 18) and the familiar right arm (M = 100.1 seconds, SD = 8). The results revealed that the aged mice spent less time in the familiar release arm than both the novel, $p < .0001$, and familiar right arm, $p < .0001$. The difference in time spent in the novel and familiar right arm was non-significant, p = .137 (figure 10d). In summary, results suggest that both young and aged LoxP-mini*Tdg* groups are less interested in exploring the familiar right arm. However, more animals need to be included in the test to improve the statistical power.

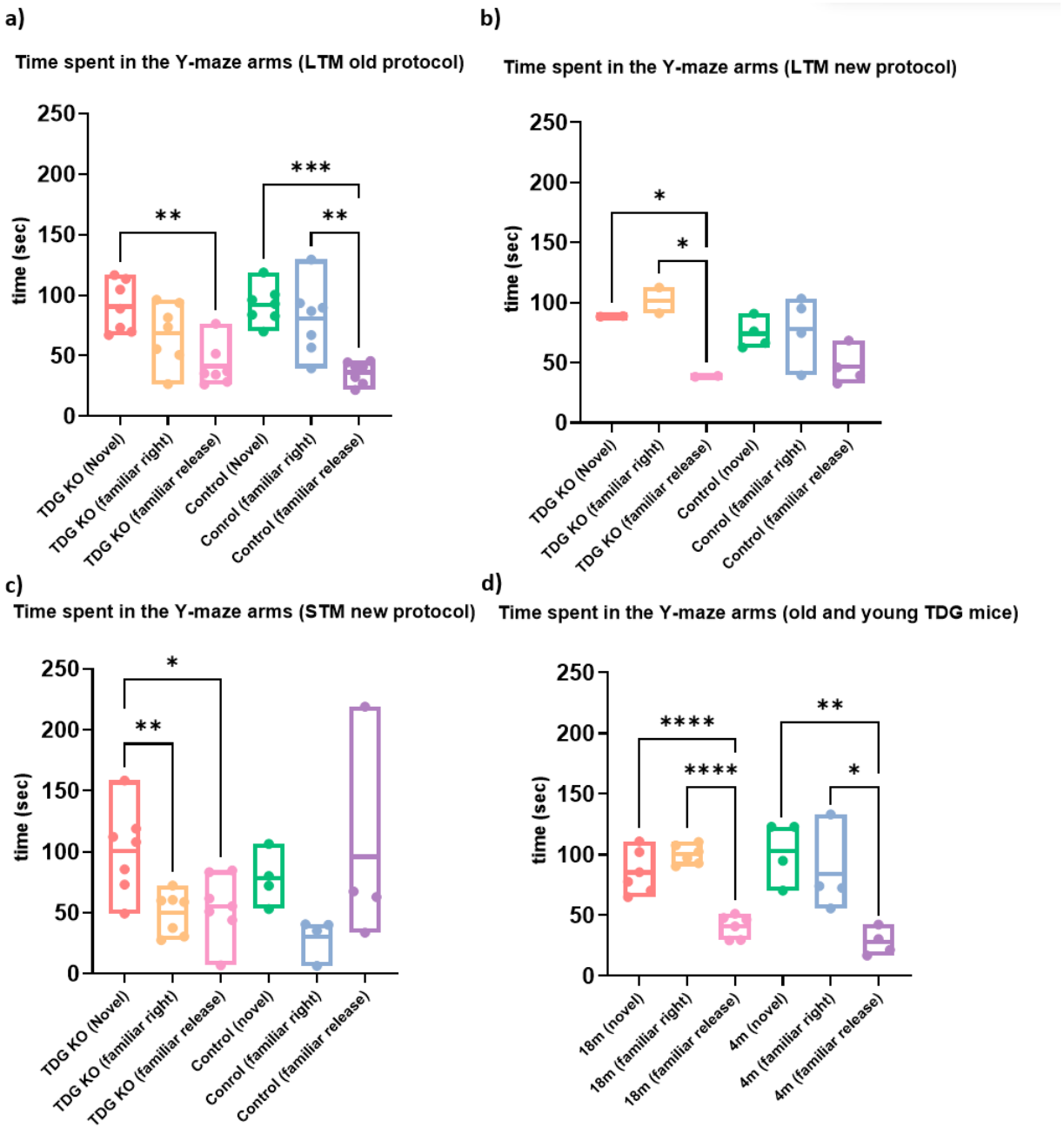

Figure 10. Total amount of time spent in novel left, familiar right, and familiar release arm in the Y-maze test. Individual mice are represented by coloured dots. Statistically significant difference between groups is determined by one-way ANOVA and post-hoc Tukey's HSD test. a) The graph shows time spent in the Y-maze arms by CamKIIα-*Tdg*$^{-/-}$ (*Tdg*-KO) (n = 7) and control mice (n = 7) when testing long term spatial memory using the old established protocol. b) The graph shows time spent in the Y-maze arms by CamKIIα-*Tdg*$^{-/-}$ (*Tdg*-KO) (n = 2) and control mice (n = 4) when testing long term spatial memory using the optimised protocol. c) The graph shows time spent in the Y-maze arms by CamKIIα-*Tdg*$^{-/-}$ (*Tdg*-KO) (n = 7) and control mice (n = 4) when testing short term spatial memory using the optimised protocol. d) The graph shows time spent in the Y-maze arms by 18-19-month-old (n = 7) and 4-month-old *Tdg* mice (n = 4) when testing long term spatial memory using the optimised protocol. * = p < .05, ** = p < .01, *** = p < .001, **** = p < 0.0001. The graphs were created in GraphPad Prism.

3.4.2.3 Determining preference for novel location by looking at percentage of entries

CamKIIα-*Tdg*$^{-/-}$ animals were subjected to the Y-maze test to determine if TDG depletion in HPC led to impairment of spatial memory. As previously mentioned, mice with normal spatial memory show novelty preference. To determine preference for novel location, percentage of entries to novel arm compared to the familiar right arm was calculated:

$$\%\ of\ entries = \frac{entries\ (novel)}{entries\ (novel) + entries\ (familiar\ right)} \times 100$$

Long term memory (old protocol)

The control group (n = 7) had more entries (% entries), above chance level (50%) in the novel location (M = 66%, SD = 7), one sample t-test $t(6) = 5.97$, $p = .001$ (figure 11a), suggesting that the control mice have normal long-term spatial memory as expected. The *Tdg*-KO group (n = 7) spent more time in the novel location compared to the control group, and showed significance above the 50% chance level (M =67.1%, SD = 7.8), one sample t-test $t(6) = 5.80$, $p = .001$ (figure 11a). Thus far, no statistically significant difference was detected between the control and *Tdg*-KO group (independent samples t-test, $t(12) = .288$, $p = .779$), which may be due to the small sample size. In summary, results suggest that the *Tdg*-KO mice do not exhibit impaired long-term spatial memory, but more animals need to be included in the test to show the statistical difference.

Long term memory (new protocol)

The control group (n = 4) had more entries (% entries) to the novel location, (M = 54.2%, SD = 5.26), but the preference was not significantly above chance level (50%), one sample t-test $t(3) = 1.60$, $p = .207$ (figure 11b), suggesting that the control mice have normal long-term spatial memory. More animals need to be included in the test to show the statistical preference above chance level. The *Tdg*-KO group (n = 2) had more entries to the novel location compared to the control (M = 56.4%, SD = 3.1), but did not show a significant preference above the 50% chance level, one sample t-test $t(1) = 2.91$, $p = .211$ (figure 11b). So far, no statistically significant difference was detected between the control and *Tdg*-KO group (independent samples t-test, $t(4) = .512$, $p = .635$), which may be due to the small sample size. In summary, results suggest that the *Tdg*-KO mice do not exhibit impaired long-term spatial memory, but more animals need to be included in the test to show statistical power.

Short term memory (new protocol)

The control group (n = 4) had more entries, significantly above chance level (50%), in the novel arm (M = 74.18, SD = 10.67), one sample t-test $t(3) = 4.53$, $p = .020$ (figure 11c), suggesting that the control mice have normal short-term spatial memory as expected. The *Tdg*-KO group (n = 7) had less entries (%) to the novel location, but still show strong significance above the 50% chance level (M = 65.5%, SD = 6.4), one sample t-test $t(6) = 6.43$, $p < .001$ (figure 11c). So far, no statistical difference was detected between the control and *Tdg*-KO groups (independent samples t-test, $t(9) = 1.714$, $p = .121$), though this could be caused by the low sample sizes. In summary, results suggest that *Tdg*-KO may exhibit impaired short-term spatial memory, though inclusion of more animals are needed to show statistical difference.

Long term memory in young and aged mice (new protocol)

The young (4-month-old) LoxP-mini*Tdg* group (n = 4) had more entries, above chance level (50%) to the novel location (M = 56.9%, SD =3.4), one sample t-test $t(3) = 4.09$, $p = .026$ (figure 11d), suggesting that the young mice have normal long-term spatial memory as expected. The aged group (18-19-months old, n = 7), had less (%) entries to the novel location compared to the young animals, and did not show significance above the 50% chance level (M = 50.4%, SD = 18.4), one sample t-test $t(6) = .126$, $p = .904$ (figure 11d). No statistical significant difference was detected between the young and aged LoxP-mini*Tdg* groups (independent samples t-test, $t(9) = 1.368$, $p = .205$), which may be due to the small sample size. In summary, these results suggest that aged mice may exhibit impaired long-term spatial memory, but the addition of more animals is needed to show statistical difference.

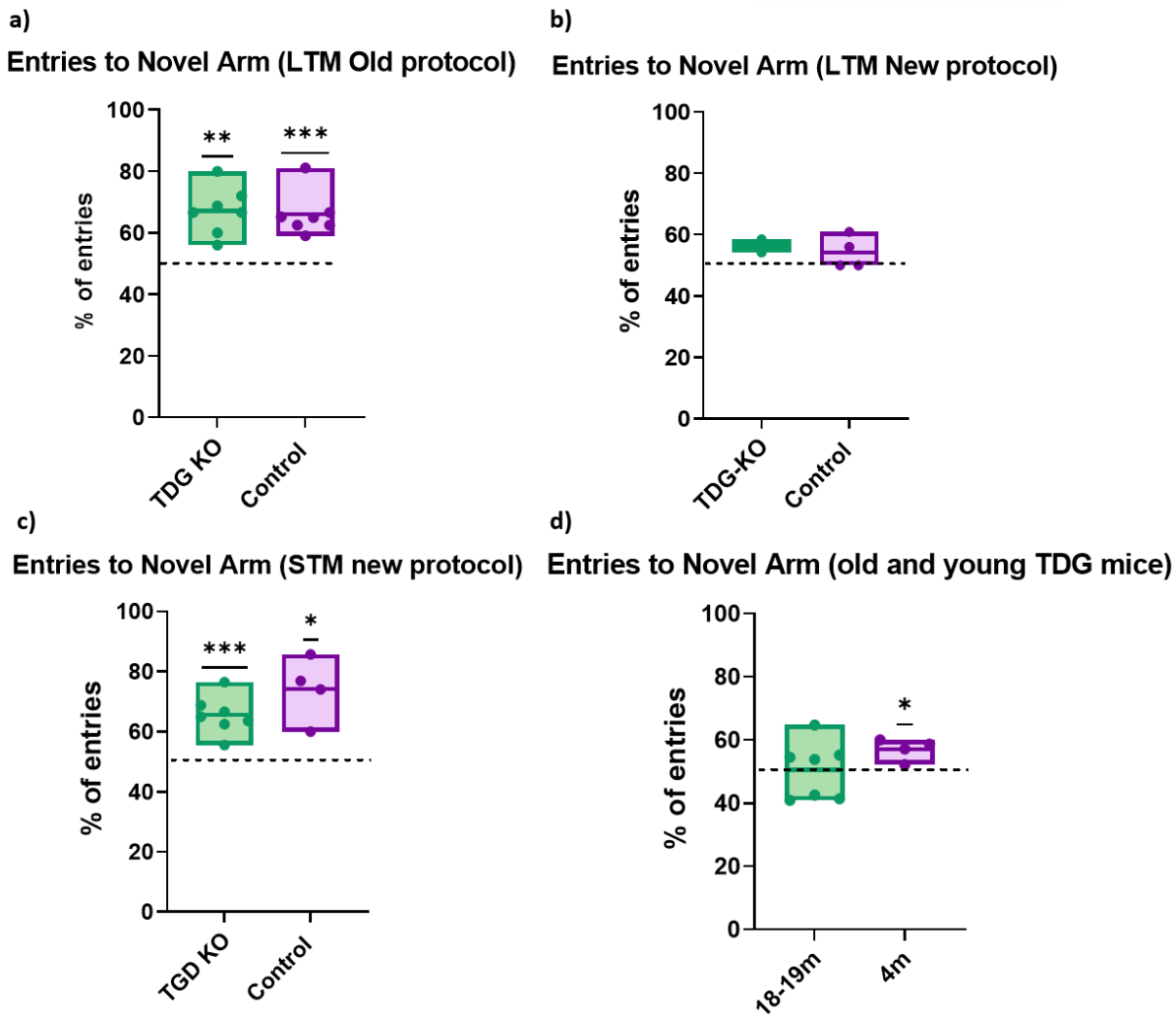

Figure 11. Percentage of entries to the novel spatial location in a Y-maze test for CamKIIα-Tdg$^{-/-}$ (Tdg-KO), control, 18-19-month-old Tdg and 4-month-old Tdg mice. Coloured dots represent individual animals. The dashed lines represent the chance level of 50%. a) The graph shows percentage of entries to the Y-maze arms by CamKIIα-*Tdg*$^{-/-}$ (*Tdg*-KO) (n = 7) and control mice (n = 7) when testing long term spatial memory using the old established protocol. b) The graph shows percentage of entries to the Y-maze arms by CamKIIα-*Tdg*$^{-/-}$ (*Tdg*-KO) (n = 2) and control mice (n = 4) when testing long term spatial memory using the optimised protocol. c) The graph shows percentage of entries to the Y-maze arms by CamKIIα-*Tdg*$^{-/-}$ (*Tdg*-KO) (n = 7) and control mice (n = 4) when testing short term spatial memory using the optimised protocol. d) The graph shows percentage of entries to the Y-maze arms by 18-19-month-old (n = 7) and 4-month-old Tdg mice (n = 4) when testing long term spatial memory using the optimised protocol. * = $p < .05$, ** = $p < .01$, *** = $p < .001$ The graphs were created in GraphPad Prism.

3.4.2.4 Determining preference for novel location by looking at percentage of time

CamKIIα-*Tdg*$^{-/-}$ animals were subjected to the Y-maze test to determine if TDG depletion in HPC led to impairment of spatial memory. As previously mentioned, mice with normal spatial memory show novelty preference. To determine preference for novel location, percentage of time spent in novel arm compared to the familiar right arm was calculated:

$$\%\ of\ time = \frac{time\ (novel)}{time\ (novel) + time\ (familiar\ right)} \times 100$$

Long term memory (old protocol)

The control group (n = 7) spent more time (% sec) in the novel location (M = 54.2%, SD = 5.2), though the preference was not above the chance level (50%), one sample t-test $t(6) = .935$, $p = .386$ (figure 12a), suggesting that the control group have normal spatial memory as expected. More animals need to be included in the test to show the statistical preference above chance level. The *Tdg*-KO group (n = 7) spent more time in novel location compared to the control, but also did not show significance above the 50% chance level (M =57.5%, SD = 13.4), one sample t-test $t(6) = 1.48$, $p = .189$ (figure 11d). So far, no statistical difference was detected between the control and *Tdg*-KO group (independent samples t-test, $t(12) = .476$, $p = .643$), which may be due to the small sample size. In summary, the results suggest that the *Tdg*-KO mice do not exibit impaired long-term spatial memory, though addition of more animals are needed to show statistical difference.

Long term memory (new protocol)

The control group (n = 4) spent around the same percentage of time (sec) as chance level (50%) in the novel location (M = 49.9%, SD = 8.56), thus the preference was not above chance level, one sample t-test, $t(3) = .03$, $p = .979$ (figure 12b), suggesting that the control group does not have normal spatial memory, which is unexpected. The *Tdg*-KO group (n = 2) spent less time in the novel location compared to control, and did not show significance above the 50% chance level (M = 46.7%, SD = 3.81), one sample t-test $t(3) = .03$, $p = .979$ (figure 12b). No statistical difference was detected between the control and *Tdg*-KO group (independent samples t-test, $t(4) = .484$, $p = .654$. In summary, the results suggest that the *Tdg*-KO mice exhibits impaired long-term spatial memory disregarding the small sample size. However, more animals are needed to show statistical difference.

Short term memory (new protocol)

The control group (n = 4) spent more time (% sec) in the novel location (M = 68.4%, SD = 18.5), but the preference was not above the chance level (50%), one sample t-test $t(3) = 1.99$, $p = .140$ (figure 12c), suggesting that the control group have normal short-term spatial memory as expected. The *Tdg*-KO group (n = 7) spent less time in the novel location compared to the control, but actually showed significance above the 50% chance level (M = 66%, SD = 11.2), one sample t-test, $t(6) = 3.78$, $p = 009$ (figure 12c). No statistical difference was detected between the control and *Tdg*-KO group (independent samples t-test, $t(9) = .266$, $p = .797$), which may be because of the small sample size. In summary, results suggest that *Tdg*-KO mice do not exhibit impaired short-term spatial memory, but we need more animals to show statistical difference.

Long term memory in young and old mice (new protocol)

The young LoxP-mini*Tdg* group (n = 4) spent more time (% sec) in the novel location (M =55.5%, SD = 12.5), but the preference was not above chance level (50%), one sample t-test $t(3) = .880$, $p = .444$ (figure 12d), suggesting that the control group have normal long-term spatial memory as expected. The aged LoxP-mini*Tdg* group (n = 7) spent less time in the novel location compared to the control group, and did not show significance above the 50% chance level (M = 50.3%, SD =13.6), one sample t-test $t(6) = .072$, $p = .945$. No statistical difference was detected between the aged and young group (independent samples t-test, $t(9) = .617$, $p = .552$), which may be due to the small sample size. In summary, results suggest that aged LoxP-mini*Tdg* mice may exhibit impaired long-term spatial memory, but we need more animals to show statistical difference.

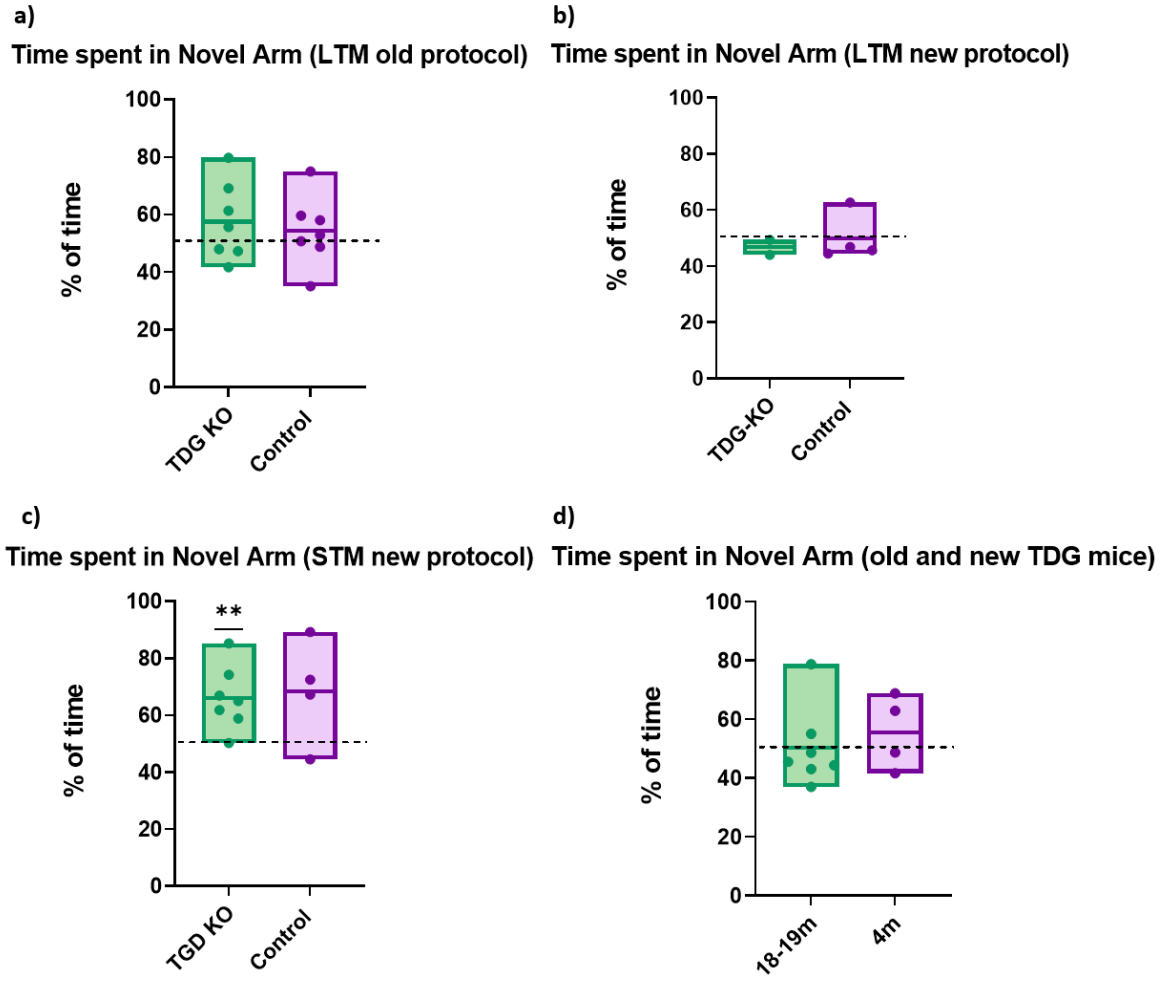

Figure 12. Percentage of time in the novel spatial location in a Y-maze test for CamKIIα-Tdg$^{-/-}$ (Tdg-KO), control, 18-19-month-old Tdg and 4-month-old Tdg mice. Coloured dots represent individual animals. The dashed lines represent the chance level of 50%. a) The graph shows percentage of time in the Y-maze arms by CamKIIα-*Tdg*$^{-/-}$ (*Tdg*-KO) (n = 7) and control mice (n = 7) when testing long term spatial memory using the old established protocol. b) The graph shows percentage of time in the Y-maze arms by CamKIIα-*Tdg*$^{-/-}$ (*Tdg*-KO) (n = 2) and control mice (n = 4) when testing long term spatial memory using the optimised protocol. c) The graph shows percentage of time in the Y-maze arms by CamKIIα-*Tdg*$^{-/-}$ (*Tdg*-KO) (n = 7) and control mice (n = 4) when testing short term spatial memory using the optimised protocol. d) The graph shows percentage of entries to the Y-maze arms by 18-19-month-old (n = 7) and 4-month-old Tdg mice (n = 4) when testing long term spatial memory using the optimised protocol. ** = $p < .01$. The graphs were created in GraphPad Prism.

4 Discussion

4.1 Wt-Tdg contamination in CamKIIα-*Tdg*$^{-/-}$ offspring

To assess the role of TDG in spatial reference memory, the mouse model CamKIIα-*Tdg*$^{-/-}$ was generated by breeding LoxP-miniTdg mice with the Tg(CamKIIα-Cre)T29 mouse strain from the Jaxson lab. This meant that the Wt-*Tdg* gene would be in some offspring, which is an undesirable gene as it cannot be excised by the cre-recombinase. Thus, carriers of Wt-*Tdg* will still have the endogenous *Tdg* gene, and therefore, there will be no functional difference in the knockout model, as the TDG protein would still be produced. Genotyping was performed by doing PCR and gel-electrophoresis to eliminate offspring with Wt-*Tdg* from further experiments. However, we started detecting Wt-*Tdg* bands in offspring of parents who had been Wt-*Tdg* negative during previous genotyping testing.

4.1.1 Critique og the methodology

When starting this project, a PCR and gel-electrophoresis protocol for testing for Wt-*Tdg* allele (along with CamKIIα promoter, mini*Tdg* allele and eGFP allele) had already been established. A gradient PCR was run to find the optimal annealing temperature for each primer pair. Therefore, we did not have reason to believe that the annealing temperature was the cause of the decrease in sensitivity of the Wt-*Tdg* primers.

In our PCR protocol, crude lysate from ear clippings of mice has been used for genotyping. The use of crude lysate for genotyping is quick and inexpensive, but it has its disadvantages. There could be contaminants and inhibitors in the lysate that could interfere with the results (111). If the lysate is too contaminated, the Wt-*Tdg* primers might not be able to specifically pick up on the targeted gene sequence. This contamination problem could be solved by implementing purification of the DNA before performing PCR. Purification protocols, like organic extraction with phenol/chloroform, magnetic beads, or silica column, are designed to remove contaminators and inhibitors (111). However, such protocols can be expensive and difficult to implement on a workstation. Despite this, we performed purification of DNA by the beads extraction method, and were able to successfully detect PCR products for the Wt-*Tdg* allele. In the future, implementing a DNA purification step in our genotyping protocol could be beneficial.

4.1.2 Potential consequences of wrongfully genotyped animals

After discovering that the Wt-*Tdg* genotyping test was not as sensitive as previously assumed, we re-genotyped the already genotyped animals that were used in experiments. Some animals that were previously confirmed to be negative for the endogenous Wt-*Tdg* gene were later discovered to be Wt-*Tdg* positive. Consequently, this led to the continuation of the endogenous Wt-*Tdg* gene to be passed on to later generations. In addition, we had to confirm genotypes of animals that had been used in other experiments (like behaviour, staining and cellular recordings), as a precaution to exclude them from results. To increase the reliability of the results, we repeated the PCR and gel-electrophoresis on purified DNA extract from experimental animals. Fortunately, only two of the animals used in other experiments were determined to be Wt-*Tdg* positive. These animals were removed from experiments.

4.2 Assessing hippocampal Cre-induced GFP expression in CamKIIα-*Tdg*$^{-/-}$ mice

As previously mentioned, we used the conditional knockout mouse model CamKIIα-*Tdg*$^{-/-}$ to determine the role of TDG in hippocampal-dependent memory formation. The CamKIIα promoter primarily expresses Cre in the pyramidal layer of CA1 (96), which is why we expect knockout to occur in this area. To investigate where *Tdg* knockout had occurred, we performed immunohistochemistry (IHC) with GFP and NeuN antibodies of brain sections from six 3-4-month-old CamKIIα-*Tdg*$^{-/-}$ mice who had gone through behaviour tests to observe GFP expression. This was done to determine the proportion of neurons in the HPC that had experienced *Tdg* knockout.

4.2.1 Main findings

Axioscan showed GFP expression in the HPC areas of CA1, CA3, and DG in CamKIIα-*Tdg*$^{-/-}$ mice. By quantifying GFP and NeuN positive cells in IMARIS using confocal images, we found that the proportion of Cre-induced GFP positive neurons was highest in CA1, with a mean percentage of GFP positive cells at 85.3%. As we know the CamKIIα promoter is predominantly expressed in CA1, these results are not surprising. The proportion of GFP % neurons was at 66.3% in DG and 45.5% in CA3, indicating *Tdg* knockout in these areas as well.

4.2.2 Critique of the methodology

Using a conditional knockout mouse model for TDG depletion has many benefits. Fist of all, it allows for the knockout to be more controlled, as we are using a time and tissue specific promotor for cre expression. As genes can have a variety of functions and roles depending on the tissue they are expressed in, conditional knockout gives us an accurate picture of gene function in a specific tissue. In addition, the problem of embryonic lethality is solved, as the knockout does not occur until p20. Another method often used to perform conditional knockout, is delivery of Cre via viral tools. This method is more expensive and more invasive than creating a mouse model. The surgeries needed to introduce Cre are time consuming, which is another downside. Therefore, the use of CamKIIα-*Tdg*$^{-/-}$ conditional knockout mouse model reaps many benefits.

The creation of CamKIIα-*Tdg*$^{-/-}$ mice is also a time-consuming process, and many animals are needed. However, when the strain is first generated, a lot of time is saved. Another downside is the expression pattern of the CamKIIα promoter. As it is predominantly active in CA1, other areas in the HPC regions, like DG and CA3, does not experience full *Tdg* knockout. This is observed in our results, as the proportion of GFP positive cells in the DG and Ca3 are less than 70%. Thus, there is not an even *Tdg* knockout in the HPC, which could impact our behaviour results. Lastly, the specificity of the CamKIIα promoter controlling expression of Cre is essential for conditional *Tdg* knockout. Expression of Cre can be leaky, which results in widespread recombination. This can lead to deletion of floxed genes in the germline of Cre-mouse lines, which in turn may result in the knockout allele hereditably remaining in offspring (112).

The antibodies used in the IHC experiments were GFP and NeuN. The reason we use GFP antibodies is to visualise GFP expression in the tissues, as GFP expression is an indicator of *Tdg* knockout. This is because Cre not only excises mini*Tdg*, but also a stop codon before an eGFP sequence. NeuN antibodies are used to detect NeuN, which is a marker for postmitotic neurons (113). This combination of antibodies together enables observation of neurons and GFP positive cells at the same time, which makes quantifying GFP positive

cells straightforward. However, as we are using GFP antibodies, we can only assume *Tdg* knockout, not fully confirm it. Other methods would be required to do so. For example, we could use TDG antibodies to observe *Tdg* expression in tissues.

4.3 Assessing anxiety of CamKIIα-*Tdg*$^{-/-}$ mice

To assess spatial memory in CamKIIα-*Tdg*$^{-/-}$ mice, the animals were subjected to behavioural tests. One of these tests, open field test (OFT), is used to assess the anxiety levels of mice. The reason for this is that high levels of stress and anxiety in mice can impact the performance on the behaviour tests. Anxious mice may spend most of their time in the corners of the maze and refuse to explore the environment, which will inevitably impact their performance in other behavioural tasks. We wanted to investigate if the newly generated mouse strain CamKIIα-*Tdg*$^{-/-}$ had elevated anxiety levels. In addition, we investigated the anxiety levels of LoxP-mini*Tdg* mice, as these were used in the control group. The anxiety of young and aged LoxP-mini*Tdg* mice were also investigated, as these animals were used to review the optimised behaviour protocol.

4.3.1 Main Findings

Based on the results, the CamKIIα-*Tdg*$^{-/-}$ mice did not exhibit any elevated form of anxiety compared to the control group. The aged (18-19-month-old *Tdg*) and young (4-month-old) LoxP-mini*Tdg* mice did not exhibit elevated anxiety levels.

4.3.2 Critique of the methodology

The use of the OFT to assess anxiety-related behaviour in rodents has many benefits, and the test is widely used and well characterised (108). Firstly, the test itself is easy to conduct, as it does not require extensive training for the examiner, nor is it time-consuming. Secondly, it does not expose the animals to any physical harm, and the test is not associated with extensive stress. At the beginning of this project, the protocol involved lifting the mice gently by the tail into the maze. Studies show that this type of handling can be a major source of handling stress for mice. It can also lead to the mice having aversion to the handler (114). After protocol optimisation, the use of red tunnels to transport the animals from cages to the mazes was implemented. Studies have found that the use of red tunnels to lift mice greatly reduces anxiety in mice, compared to the method of lifting them by their tail (115). Even though there were no notable changes in OFT performance after the tunnels were implemented, subjectively, the handler experienced the mice to be less averse to their presence.

Even though there are many advantages to using the OFT, there are some disadvantages as well. The OFT we used primarily investigates time spent in corner zones and the centre zone as a way of assessing anxiety. In addition, the ANY-Maze programme also records distance travelled and velocity in the zones during the OFT, though this data was not used to assess anxiety. There are other ways of assessing anxiety related behaviour, like observation of quivering movements, gnawing on walls, or amount of animal excrement (116), and these factors have not been considered when using the OFT. However, these measurements are based on subjective observations. Theoretically, even though an animal spent most of its time in the centre, it might have been frozen or shivering the whole time, suggesting elevated anxiety and stress. Another disadvantage the OFT shares with most other behavioural tests, is the possibility of external factors influencing the animals' behaviour. Even though olfactory, auditory and visual ques were kept to a minimum in a

controlled environment, there is a possibility that deviations in such stimuli influences the animals' behaviour (117), resulting in the behaviour being incorrectly interpreted.

4.3.3 Reliability and relevance of the results

So far, there have been no published studies investigating anxiety levels in mice with hippocampal-dependent TDG depletion to our knowledge. However, anxiety in gene knockout models have been studies. Therefore, our results can be somewhat compared to any previously published behaviour studies.

We found that the CamKIIα-*Tdg*$^{-/-}$ mice spent a similar amount of time in the corner zones compared to the centre zone, though this difference was not significant. Meanwhile, the results showed that the LoxP-mini*Tdg* mice used in the control group spent significantly more time in the corners than in the centre. However, no significant difference were detected between the groups. These results are somewhat surprising, as mice experiencing knockout of genes involved in memory formation have been shown to exhibit increased levels of anxiety by previous studies (118). There are several possible explanations for our results. The high variance (*SD*) in the groups, even after outliers were removed, could be a possible explanation why there were no significant difference between the groups. In addition, the sample sizes of the groups are different, due to removal of outliers and removal of Wt-*Tdg* positive mice from the test. Not only is the sample sizes different, the sample sizes are also relatively small. This might explain the difference in statistical results.

Our results also showed that both aged (18-19-month-old) and young (4-month-old) LoxP-mini*Tdg* mice did not exhibit increased anxiety-related behaviour. However, the small sample size in each group, especially for the young mice, lessens the reliability of these results. In addition, there is a difference in the sample size between the aged and young mice. A small sample size makes it difficult to determine if the outcome of these results is a true finding or not. This is a recurring theme throughout our later behaviour results.

4.4 Assessing functional spatial memory in CamKIIα-*Tdg*$^{-/-}$ animals

Transcription of genes associated with memory formation is essential for long term synaptic plasticity and long term memory formation (119). The epigenetic mechanisms of DNA methylation and demethylation influence the transcription of these genes (120). This suggests that regulation of these pathways and contributing factors actively involved in the pathways are essential for memory formation. As TDG is a contributing enzyme in DNA demethylation, we hypothesize that TDG plays a role in the formation of long-term memory. Unlike short-term memory (working memory), long-term memory formation is dependent upon transcription of genes whose products are needed for the formation of memory (121). This process takes time, which is why we assume TDG depletion mostly affects long-term memory as TDG is implicated in transcriptional regulation. Therefore, we wanted to investigate whether hippocampal depletion of TDG affects long-term and short-term memory, by subjecting CamKIIα-*Tdg*$^{-/-}$mice to behavioural tests. In addition, optimisation of behavioural protocols was performed to improve the procedure.

4.4.1 Main Findings

The main aim of this study was to investigate if depletion of TDG in the HPC impacted long-term spatial memory. In addition to subjecting CamKIIα-*Tdg*$^{-/-}$ mice to behavioural tasks

testing long term spatial memory, we also tested short term memory. A group of LoxP-mini*Tdg* mice were used as a control group. Also, aged and young LoxP-mini*Tdg* mice were subjected to tests investigating long term memory, to assess our protocol. Results from the different behaviour tests were contradictive. Therefore, it is not apparent whether depletion of TDG in the HPC affects spatial memory. However, some behaviour results indicated that long-term spatial memory was somewhat impaired in CamKIIα-*Tdg*$^{-/-}$ mice, compared to control.

In addition, we wanted to investigate whether optimisation of the behaviour protocol (Y-maze) led to animals being inspired to explore the familiar right and novel arm instead of the familiar release arm. Our results reveal some indications that the optimisation of the behaviour protocols led to the mice being more interested in novel and familiar right arm compared to the familiar release arm.

4.4.2 Choice of behaviour tests

The NOL test is commonly used to assess cognition and health of certain brain regions involved in learning and memory (88). Mice inherently have a preference and curiosity to novel objects or novel locations, which is something the NOL test exploits to assess spatial memory. As we are testing if hippocampal-dependent memory is affected by *Tdg* knockout, a test assessing spatial memory is ideal, as this memory function is heavily associated with the HPC (83). Spatial cues are attached to the environment of the test, as a presence of spatial cues is needed for the animals' ability to orient themselves in an environment. In these test conditions, the NOL test is a reasonable test to use when trying to answer our research question. The Y-maze test can also be used to assess spatial memory, as in this test, the animals are given a choice between a novel and familiar location. As previously mentioned, rodents have an instinct to explore novelties compared to familiarities. By attaching spatial cues, the animals can orient themselves in the environment.

4.4.3 Critique of the methodology

The use of the NOL test and Y-maze test to assess spatial memory has many benefits. One strength is that both are already well established and well known. Another strength is that neither test require extensive training for the experiment conductor, neither is the test exceedingly time consuming. Food deprivation or external reinforcements are not needed to perform these tests, nor negative reinforcement. In addition, the animals are not subjected to pain or stressful situations that can cause them anxiety, like in the Morris water maze or fear conditioning test.

Though there are many benefits using these behaviour tests, there are some weaknesses as well. First, the tests rely on the mice having a willingness to explore the environment. Anxiety-related behaviour, like freezing, can influence the willingness to explore. There might be individual differences in exploration interest and activity levels, which can result in a large variance within groups. We perform an OFT so that animals who are evidently anxious are taken into consideration when analysing the behaviour test results. Another weakness of this study is that the memories created in these tests are not as strong as memories created when negative or positive reinforcements are used. Mice are not penalised for not entering the correct location, compared to in fear conditioning tests, where pain is introduced to the animal, creating a strong memory. This is because receiving pain is is critical for the animals' survival. Lastly, the presence of external cues, like olfactory cues etc. might influence the behaviour of the mice. This was previously discussed in the OFT critique of the methodology section.

When using the Y-maze test, we initially investigate time and entries to the novel location, calculated to a percentage of novel arm exploration based on the time and entries to the novel familiar right arm. However, it is important to note that the release arm is also a familiar location for the animals. As previously stated, we worried that the interest and exploration activity of the mice were low. To combat this, we placed identical objects at the end of the novel and right arm, as we hoped this would pique their interest and exploration activity, as well as help them distinguish the release arm from the familiar right and novel left arm. (122). The objects placed were thought to be short enough so that the mice would not climb on them and jump out of the maze. However, this was proven to be false, as four mice used the objects as a jumping board to escape the maze during the test. This led to the removal of these mice from the tests, lowering the sample size of some groups. We replaced the objects with other objects with a lower height, and thus far, no mouse has jumped over the walls.

4.4.4 Reliability and relevance of the NOL test

In this study, I found that both CamKIIα-*Tdg*$^{-/-}$ and LoxP-mini*Tdg* mice preferred to explore the novel object location above chance level when using the long-term conditions. We know from previous studies that normal mice prefer to explore novelty objects/areas (123). The fact that the control group behaved as expected, suggests that the behavioural paradigm worked. The fact that the *Tdg*-KO group preferred the NOL above chance level, indicates that they do not have impaired long-term spatial reference memory. However, they spent slightly less time in NOL compared to the control (not significant, ns). These results do not support our hypothesis, as we expected impaired long-term spatial memory in these animals. There are some possible explanations to why we do not observe significant long-term spatial memory impairments in the *Tdg*-KO mice. As previously mentioned, the memories associated with NOL are not considered very strong. In comparison, a memory associated with a critical/essential event related to the survival of the species, like application of pain or contribution of treats, are more "easily remembered". The fact that there is a low sample size in each group, and that the sample sizes are different between the *Tdg*-KO and control group, questions the reliability of the results as well. To strengthen the study and increase statistical power, more animals are needed in each group.

When testing for short-term memory in NOL, our results showed that both CamKIIα-*Tdg*$^{-/-}$ and LoxP-mini*Tdg* mice exhibited no significant preference for the novel location but alternated between exploring the two objects 50/50. This is surprising, as we expect the control group to have intact short-term memory and prefer NOL. In addition, we did expect the *Tdg*-KO mice to show novelty preference, as the machinery responsible for long-term and short-term memory are different, and we hypothesise that the working memory should not be influenced. The fact that the control mice did not behave as expected, suggests that the test did not work. This could be for example be caused by handling issues or other external factors, like olfactory cues. The fact that there is a low sample size in each group, and that the sample sizes are different between the *Tdg*-KO and control group, questions the reliability of the results as well.

18-19-month-old (aged) and 4-month-old (young) LoxP-mini*Tdg* were also subjected to the NOL test. This was mainly to get familiarised with the use of red tunnels as a way of transporting the mice from cages to the maze. Simultaneously, we investigated whether there was any impairment in aged mice when it comes to long term memory, previous studies have shown that aged mice exhibits a decline in spatial memory (110,124). Our results showed that both aged and young mice preferred the NOL, suggesting no impairment in long-term spatial memory in the aged mice. These results are not in

accordance with previously published results. A possible explanation could be that ageing and senescence are diverse processes and differ from individual to individual. In addition, the fact that there is a low sample size in each group, and that the sample sizes are different between the aged and young LoxP-mini*Tdg* mice, also questions the reliability of the results. More animals are needed for testing to improve the statistical power.

4.4.5 Reliability and relevance of the Y-maze test

4.4.5.1 Optimisation of the protocol

In this study, changes were made to the already established Y-maze protocol for optimisation. The established protocol had six days of habituation to the Y-maze, followed by test day on day 7. A narrower Y-maze was used when the framework and procedure of the behaviour protocols were established, and the long habituation was needed as the narrow spaces were stressful for the mice. Today, a wider Y-maze is used. Therefore, our first optimisation point was to shorten the habituation days. In this way, the Y-maze test was on day 4, the same day as for the NOL test. This did not increase the anxiety levels in the mice. This also shortens the whole behaviour test process, from 10 days (3 days handling habituation plus 7 days maze habituation plus test) to 7 days total. Thus, the behaviour test process is more time efficient.

Another optimisation point was the addition of identical objects in the novel and familiar right arm. This was done to increase the explorative behaviour and inspire the mice to primarily tour the right and left maze arm. Our results showed that before optimisation, both control and *Tdg*-KO mice had less entries to the familiar right arm than to the familiar release arm, when testing for LTM. This is not ideal, as we compare entries to the novel and familiar right arm, and not the familiar release arm. After protocol optimisation, our results did not display any significant trends in entries to either of the three arms when testing for LTM, though we did observe some tendency to enter the familiar release arm less than the other arms. Unfortunately, the sample sizes in the groups were very low, due to time limitations on the project, as well as the post-test exclusion of two mice in the *Tdg*-KO group after Wt-*Tdg* confirmation. When testing for STM using the optimised protocol, strangely, the *Tdg*-KO group had significantly more entries to the familiar release arm. However, in this instance, it is worth to note the large variance within the group. The standard deviation in familiar release arm is more than five times as large as the standard deviation in novel and familiar right arm. This decreases the reliability of the results. Lastly, we did not observe any preference to any of the Y-maze arm when investigate the number of entries the aged and young LoxP-mini*Tdg* mice had to each arm. In summary, it is difficult to conclude anything from these results. There is not strong evidence suggesting that there is increased exploratory behaviour to the novel and right arm mice after protocol optimisation. The sample sizes in each of the groups are very low, and the sample sizes differs between the groups. This decreases the reliability of the results. As previously mentioned, a small sample size makes it difficult to determine if the outcome of these results is a true finding or not. The addition of more animals is needed to confirm if the optimisation of the protocol had any impact on the animals exploratory and distinction between the familiar right and release arm.

Another parameter considered when looking at the exploration activity in Y-maze, is the amount of time spent in each arm. The addition of identical objects was implemented in hope that animals would have increased exploratory behaviour and spend more time in the novel and familiar right arm, compared to familiar release arm. Our results showed that before optimisation, both *Tdg*-KO and control groups seemed to already spend less time in

the familiar release arm than in the other arms when testing for LTM. After protocol optimisation, the same tendency was seen in both strains when testing for LTM. When testing for STM using the optimised protocol, The *Tdg*-KO animals also spent less time in the familiar release arm than the other two, although these results were not seen in the control animals. We also observed that both the aged and young LoxP-mini*Tdg* mice spent less time in the familiar release arm compared to the other arms when testing for LTM using the optimised protocol, and this difference was significant. Disregarding the small sample size, most animals spent less time in the familiar release arm when testing for STM and LTM and independently of group. However, these observations cannot be contributed to the optimisation of the protocol, as mice already spent less time in the familiar release arm before the changes were implemented. In addition, time might not be a good indicator for novel preference. The total amount of time spent in the arms also includes time spent grooming and relaxing, as well as active exploration. The reliability of the results is also inadequate, due to the low sample size and difference in sample sizes. This problem has already been discussed, as it is a recurring problem in these tests. In addition, if mice decide to spend less time and/or have less entries to the familiar release arm, this could be caused by another factor than exploration activity. As the animals are released in the release arm, they could be associating this arm with a stressful and anxiety-inducing experience and avoid the arm accordingly. In summary, we cannot say with confidence that the addition of objects in novel and right arm increased the interest and exploration activity to these arms when observing the time variable. Perhaps, rather than placing objects in the novel and familiar right arm, the entries/time in the familiar release arm may be taken into consideration when investigating novel preference when using the Y-maze test.

4.4.5.2 Preferance to the novel location compared to chance level

In this study, I examined novelty preference in both CamKIIα-*Tdg*$^{-/-}$ and LoxP-mini*Tdg* mice as an indicator for spatial memory impairments. As previously mentioned, we know that normal mice prefer to explore novelties (123) and mice with normal spatial memory should have spatial novelty preference. In this study, the results from entries to the novel arm and time spent in the novel arm were contradictory. When testing animals in the long-term conditions using the established protocol, CamKIIα-*Tdg*$^{-/-}$ and LoxP-mini*Tdg* mice preferred to explore the novel location above chance level when considering investigating percentage of entries to the novel arm. However, when observing percentage of time spent in the novel location, our results indicated that both the *Tdg*-KO and control group randomly alternated between the arms. As the control animals did not behave as expected, this indicates that the test did not work, and we cannot confidently ascertain whether the *Tdg*-KO experience memory impairments or not. As previously stated, the sample sizes in the groups tested in long-term conditions using the optimised protocol are considerably small. Therefore, we are not able to determine any preference for the novel location, notwithstanding the entries or time variables. The addition of more animals is needed to be able to observe any statistically significant difference between control and *tdg*-KO animals.

When observing the Y-maze results in the short-term condition using the optimised protocol, the percentage of entries to novel location suggests that both control and *Tdg*-KO have a novelty preference, and that this preference was statistically significant. The results from the control animals are in accordance with literature, as normal mice have a novelty preference. The *Tdg*-KO have less percentage entries to novel arm compared to the control, but this difference was not significant. The fact that the *Tdg*-KO animals show

novelty preference indicates that they have intact short-term memory. This is in accordance with our hypothesis, as we only expected long-term spatial memory to be affected. When observing the percentage of time spent in the novel arm, both groups show preference to the novel location, though this preference is only significant in the *Tdg*-KO group.

In this study, the results based on percentage of entries found that only young and not aged LoxP-mini*Tdg* mice showed a significant preference to the novel arm. The results based on percentage of time in the novel arm suggest that neither young nor aged LoxP-mini*Tdg* mice have any preference to the novel arm. This is surprising, as the young group should have intact long-term spatial memory. These results are probably not reliable, due to the small sample size and the difference in sample size between the groups.

Most often, the observation of percentage of entries are used as a variable when investigating Y-maze results (125,126). If only taking into consideration the results based on entries, our findings indicate that CamKIIα-*Tdg*$^{-/-}$ most often prefer the novel location above chance level, though in some occasions show less preference than the control group. However, the sample sizes of the groups are very small, and a large sample size must be included to confirm these results.

4.4.6 Conditional knockout model and behaviour results

As previously mentioned, our results showed that presumable *Tdg* knockout occurred in 85% of neurons in CA1, 66% of neurons in DG, and 45% of neurons in CA3 in CamKIIα-*Tdg*$^{-/-}$. This suggests that most of the neurons in HPC experience knockout, though not all. The fact that we have not detected 100% GFP expression in HPC could help explain why we do not detect any statistically significant difference between *Tdg*-KO and control groups in any of the behaviour tests investigating spatial memory impairment. Another possible reason for not observing definite spatial memory impairments in *Tdg*-KO mice could be that there is a form for compensation of the TDG function from other enzymes. However, this is just speculation.

5 Conclusion

In this study, I managed to determine the portion of neurons expressing GFP in the CA1, CA3 and DG of CamKIIα-*Tdg*$^{-/-}$ mice, thereby determining the portion of neurons with presumable TDG depletion. My findings showed that a majority of the knockout occurred in CA1, where over 80% of the neurons were GFP positive. Further, I subjected CamKIIα-*Tdg*$^{-/-}$ animals to behaviour tests to investigate whether TDG depletion in hippocampal neurons anxiety and spatial memory. No increase in anxiety were detected in the CamKIIα-*Tdg*$^{-/-}$ and LoxP-mini*Tdg* animals. A portion of animals were tested in NOL and Y-maze long-term conditions before I implemented changes to the behaviour protocol for optimisation and investigated the effects. After optimisation, there was some indication that animals were less interested in exploring the familiar release arm compared to novel and familiar right arm based on total number of entries, though a larger sample size is needed to conclude any findings. However, the addition of red tunnels and reduction of maze habituation days were deemed to be successful. It is not clear whether hippocampal TDG depletion affects long-term spatial memory, as several behaviour results were contradictory, though some test results implied that CamKIIα-*Tdg*$^{-/-}$ animals exhibited a tendency to prefer novel location preference less than the LoxP-mini*Tdg* animals. However, a larger sample size is needed to conclude any findings and improve statistical power. In addition, we observed some indications that the aged (18-19-month-old) LoxP-mini*Tdg* had impaired spatial memory compared to the young LoxP-mini*Tdg* mice, though more animals need to be included in the test to show statistical significance.

6 Future Perspectives

To continue the investigation of TDGs role in hippocampal-dependent memory, additional tests should be performed. Several studies would be interesting to implement:

1. As GFP expression in CamKIIα-*Tdg*$^{-/-}$ mice is not confined to the HPC region alone, quantifying the portion of GFP positive cells in other regions where GFP expression is observed, like subiculum and medial entorhinal cortex, could be performed. In this way, we can determine if there is Cre expression and presumable *Tdg* knockout in these regions as well.

2. Purification of DNA from animals intended for other experiments should be performed before PCR and gel-electrophoresis in genotyping, as this was shown to increase detectability of Wt-*Tdg*.

3. To determine if *Tdg* knockout in the CamKIIα-*Tdg*$^{-/-}$ mouse model has been successful, we could use fluorescence-activated cell sorting (FACS) to cultivate GFP positive cells from the hippocampal regions. This could be followed by the use of western blot (WB) to detect TDG protein and RT-PCR to detect mini*Tdg* mRNA to estimate if TDG depletion has been successful.

4. A study by Schwarz et al. found that embryonic stem cells with TDG depletion had accumulation of the 5fC and 5caC, which are recognised by TDG, but no accumulation of 5hmC, which is not recognised by TDG (104). It would therefore be interesting to use Mass Spectrometry (MS) to measure the levels of 5mC, 5hmC, 5fC and 5caC in the HPC.

5. To continue the investigation on the effects of protocol optimisation, more animals could be included in the y-maze test. By doing so, statistical power would be increased, and the results would be more reliable. Moreover, more CamKIIα-*Tdg*$^{-/-}$ mice could be added in the NOL test as well to increase reliability of behaviour results.

6. Other behavioural paradigm associated with stronger memory generation could be included to better understand the role of TDG mediated DNA demethylation in memory. Some examples of tests we could implement in our lab, are the fear conditioning test, and radial arm maze. These tests share that they implement (negative or positive) reinforcements which may expedite the speed of learning and memory formation (127). The fear conditioning test involves assessment of the ability of rodents to lean and remember a spatial location to an aversive stimulus. Animals with impaired spatial memory will not associate the spatial location to the fear inducing stimuli, and unlike normal mice, will not demonstrate a freezing response (128). The radial arm maze test consists of a maze with eight arms, where food can be placed at the end of each arm. Visual cues help guide the animals to the location(s) with a reward. Spatial memory and working memory can be assessed by measuring the amount of errors that animals make when exploring the maze (129).

7 References

1. Eagle AL, Gajewski PA, Robison AJ. Role of hippocampal activity-induced transcription in memory consolidation. Rev Neurosci. 2016 Aug 1;27(6):559–73.

2. Fortin NJ, Agster KL, Eichenbaum HB. Critical role of the hippocampus in memory for sequences of events. Nat Neurosci. 2002 May 25;5(5):458–62.

3. Hardeland U, Bentele M, Lettieri T, Steinacher R, Jiricny J, Schär P. Thymine DNA glycosylase. In: Progress in Nucleic Acid Research and Molecular Biology. 2001. p. 235–53.

4. da Costa NM, Hautefeuille A, Cros M-P, Melendez ME, Waters T, Swann P, et al. Transcriptional regulation of thymine DNA glycosylase (TDG) by the tumor suppressor protein p53. Cell Cycle. 2012 Dec 15;11(24):4570–8.

5. Baylin SB. DNA methylation and gene silencing in cancer. Nat Clin Pract Oncol. 2005 Dec;2(S1):S4–11.

6. Lubin FD, Roth TL, Sweatt JD. Epigenetic Regulation of *bdnf* Gene Transcription in the Consolidation of Fear Memory. J Neurosci. 2008 Oct 15;28(42):10576–86.

7. Onodera A, González-Avalos E, Lio C-WJ, Georges RO, Bellacosa A, Nakayama T, et al. Roles of TET and TDG in DNA demethylation in proliferating and non-proliferating immune cells. Genome Biol. 2021 Dec 22;22(1):186.

8. Sibghat-Ullah, Gallinari P, Xu Y-Z, Goodman MF, Bloom LB, Jiricny J, et al. Base Analog and Neighboring Base Effects on Substrate Specificity of Recombinant Human G:T Mismatch-Specific Thymine DNA−Glycosylase. Biochemistry. 1996 Jan 1;35(39):12926–32.

9. Gallinari P, Jiricny J. A new class of uracil-DNA glycosylases related to human thymine-DNA glycosylase. Nature. 1996 Oct;383(6602):735–8.

10. Wiebauer K, Jiricny J. Mismatch-specific thymine DNA glycosylase and DNA polymerase beta mediate the correction of G.T mispairs in nuclear extracts from human cells. Proc Natl Acad Sci. 1990 Aug;87(15):5842–5.

11. Smet-Nocca C, Wieruszeski J-M, Chaar V, Leroy A, Benecke A. The Thymine−DNA Glycosylase Regulatory Domain: Residual Structure and DNA Binding. Biochemistry. 2008 Jun 1;47(25):6519–30.

12. Maiti A, Morgan MT, Drohat AC. Role of Two Strictly Conserved Residues in Nucleotide Flipping and N-Glycosylic Bond Cleavage by Human Thymine DNA Glycosylase. J Biol Chem. 2009 Dec;284(52):36680–8.

13. Neddermann P, Jiricny J. The purification of a mismatch-specific thymine-DNA glycosylase from HeLa cells. J Biol Chem. 1993 Oct;268(28):21218–24.

14. Malfatti MC, Antoniali G, Codrich M, Tell G. Coping with RNA damage with a focus on APE1, a BER enzyme at the crossroad between DNA damage repair and RNA processing/decay. DNA Repair (Amst). 2021 Aug;104:103133.

15. Krokan HE, Bjoras M. Base Excision Repair. Cold Spring Harb Perspect Biol. 2013 Apr 1;5(4):a012583–a012583.

16. Tini M, Benecke A, Um S-J, Torchia J, Evans RM, Chambon P. Association of CBP/p300 Acetylase and Thymine DNA Glycosylase Links DNA Repair and

Transcription. Mol Cell. 2002 Feb;9(2):265–77.

17. Wu X, Zhang Y. TET-mediated active DNA demethylation: mechanism, function and beyond. Nat Rev Genet. 2017 Sep 30;18(9):517–34.

18. Morgan MT, Bennett MT, Drohat AC. Excision of 5-Halogenated Uracils by Human Thymine DNA Glycosylase. J Biol Chem. 2007 Sep;282(38):27578–86.

19. Lim W-J, Kim KH, Kim J-Y, Jeong S, Kim N. Identification of DNA-Methylated CpG Islands Associated With Gene Silencing in the Adult Body Tissues of the Ogye Chicken Using RNA-Seq and Reduced Representation Bisulfite Sequencing. Front Genet. 2019 Apr 16;10.

20. Cortellino S, Xu J, Sannai M, Moore R, Caretti E, Cigliano A, et al. Thymine DNA Glycosylase Is Essential for Active DNA Demethylation by Linked Deamination-Base Excision Repair. Cell. 2011 Jul;146(1):67–79.

21. Cortázar D, Kunz C, Selfridge J, Lettieri T, Saito Y, MacDougall E, et al. Embryonic lethal phenotype reveals a function of TDG in maintaining epigenetic stability. Nature. 2011 Feb;470(7334):419–23.

22. Xu X, Watt DS, Liu C. Multifaceted roles for thymine DNA glycosylase in embryonic development and human carcinogenesis. Acta Biochim Biophys Sin (Shanghai). 2016 Jan 1;48(1):82–9.

23. TDG thymine DNA glycosylase [Homo sapiens (human)] [Internet]. Bethesda (MD), National Library of Medicine (US), National Center for Biotechnology Information. 2004 [cited 2023 Mar 13]. Available from: https://www.ncbi.nlm.nih.gov/gene/6996

24. Aravind L, Koonin E V. The alpha/beta fold uracil DNA glycosylases: a common origin with diverse fates. Genome Biol. 2000;1(4):research0007.1.

25. Sjolund AB, Senejani AG, Sweasy JB. MBD4 and TDG: Multifaceted DNA glycosylases with ever expanding biological roles. Mutat Res Mol Mech Mutagen. 2013 Mar;743–744:12–25.

26. Uhlén M, Fagerberg L, Hallström BM, Lindskog C, Oksvold P, Mardinoglu A, et al. Tissue-based map of the human proteome. Science (80-). 2015 Jan 23;347(6220).

27. Missero C, Pirro MT, Simeone S, Pischetola M, Di Lauro R. The DNA Glycosylase T:G Mismatch-specific Thymine DNA Glycosylase Represses Thyroid Transcription Factor-1-activated Transcription. J Biol Chem. 2001 Sep;276(36):33569–75.

28. Um S, Harbers M, Benecke A, Pierrat B, Losson R, Chambon P. Retinoic Acid Receptors Interact Physically and Functionally with the T:G Mismatch-specific Thymine-DNA Glycosylase. J Biol Chem. 1998 Aug;273(33):20728–36.

29. Chen D, Lucey MJ, Phoenix F, Lopez-Garcia J, Hart SM, Losson R, et al. T:G Mismatch-specific Thymine-DNA Glycosylase Potentiates Transcription of Estrogen-regulated Genes through Direct Interaction with Estrogen Receptor α. J Biol Chem. 2003 Oct;278(40):38586–92.

30. Tdg thymine DNA glycosylase [Mus musculus (house mouse) [Internet]. Bethesda (MD), National Library of Medicine (US), National Center for Biotechnology Information. 2004 [cited 2023 Mar 13]. Available from: https://www.ncbi.nlm.nih.gov/gene/21665

31. Kohli RM, Zhang Y. TET enzymes, TDG and the dynamics of DNA demethylation. Nature. 2013 Oct 23;502(7472):472–9.

32. Wu C -t., Morris JR. Genes, Genetics, and Epigenetics: A Correspondence. Science

(80-). 2001 Aug 10;293(5532):1103–5.

33. Portela A, Esteller M. Epigenetic modifications and human disease. Nat Biotechnol. 2010 Oct 13;28(10):1057–68.

34. Tsankova N, Renthal W, Kumar A, Nestler EJ. Epigenetic regulation in psychiatric disorders. Nat Rev Neurosci. 2007 May;8(5):355–67.

35. Moore LD, Le T, Fan G. DNA Methylation and Its Basic Function. Neuropsychopharmacology. 2013 Jan 11;38(1):23–38.

36. Lyko F. The DNA methyltransferase family: a versatile toolkit for epigenetic regulation. Nat Rev Genet. 2018 Feb 16;19(2):81–92.

37. Dantas Machado AC, Zhou T, Rao S, Goel P, Rastogi C, Lazarovici A, et al. Evolving insights on how cytosine methylation affects protein-DNA binding. Brief Funct Genomics. 2015 Jan 1;14(1):61–73.

38. Stirzaker C, Song JZ, Davidson B, Clark SJ. Transcriptional Gene Silencing Promotes DNA Hypermethylation through a Sequential Change in Chromatin Modifications in Cancer Cells. Cancer Res. 2004 Jun 1;64(11):3871–7.

39. Belinsky SA. Silencing of genes by promoter hypermethylation: key event in rodent and human lung cancer. Carcinogenesis. 2005 Sep 1;26(9):1481–7.

40. Herman JG, Baylin SB. Gene Silencing in Cancer in Association with Promoter Hypermethylation. N Engl J Med. 2003 Nov 20;349(21):2042–54.

41. Unoki M. Recent Insights into the Mechanisms of *De Novo* and Maintenance of DNA Methylation in Mammals. In: DNA Methylation Mechanism. IntechOpen; 2020.

42. Okano M, Bell DW, Haber DA, Li E. DNA Methyltransferases Dnmt3a and Dnmt3b Are Essential for De Novo Methylation and Mammalian Development. Cell. 1999 Oct;99(3):247–57.

43. Chen B-F, Chan W-Y. The de novo DNA methyltransferase DNMT3A in development and cancer. Epigenetics. 2014 May 6;9(5):669–77.

44. Zhang W, Xu J. DNA methyltransferases and their roles in tumorigenesis. Biomark Res. 2017 Dec 20;5(1):1.

45. Xiao F-H, Wang H-T, Kong Q-P. Dynamic DNA Methylation During Aging: A "Prophet" of Age-Related Outcomes. Front Genet. 2019 Feb 18;10.

46. Murgatroyd C, Patchev A V, Wu Y, Micale V, Bockmühl Y, Fischer D, et al. Dynamic DNA methylation programs persistent adverse effects of early-life stress. Nat Neurosci. 2009 Dec 8;12(12):1559–66.

47. Ziller MJ, Gu H, Müller F, Donaghey J, Tsai LT-Y, Kohlbacher O, et al. Charting a dynamic DNA methylation landscape of the human genome. Nature. 2013 Aug 7;500(7463):477–81.

48. Bogdanovic O, Vermeulen M. Correction to: TET Proteins and DNA Demethylation. In 2021. p. C1–C1.

49. Wu SC, Zhang Y. Active DNA demethylation: many roads lead to Rome. Nat Rev Mol Cell Biol. 2010 Sep 4;11(9):607–20.

50. Pecori R, Di Giorgio S, Paulo Lorenzo J, Nina Papavasiliou F. Functions and consequences of AID/APOBEC-mediated DNA and RNA deamination. Nat Rev Genet. 2022 Aug 7;23(8):505–18.

51. Hegde ML, Hazra TK, Mitra S. Early steps in the DNA base excision/single-strand interruption repair pathway in mammalian cells. Cell Res. 2008 Jan 1;18(1):27–47.

52. Ito S, Shen L, Dai Q, Wu SC, Collins LB, Swenberg JA, et al. Tet Proteins Can Convert 5-Methylcytosine to 5-Formylcytosine and 5-Carboxylcytosine. Science (80-). 2011 Sep 2;333(6047):1300–3.

53. Guo JU, Su Y, Zhong C, Ming G, Song H. Hydroxylation of 5-Methylcytosine by TET1 Promotes Active DNA Demethylation in the Adult Brain. Cell. 2011 Apr;145(3):423–34.

54. He Y-F, Li B-Z, Li Z, Liu P, Wang Y, Tang Q, et al. Tet-Mediated Formation of 5-Carboxylcytosine and Its Excision by TDG in Mammalian DNA. Science (80-). 2011 Sep 2;333(6047):1303–7.

55. Day JJ, Sweatt JD. DNA methylation and memory formation. Nat Neurosci. 2010 Nov 26;13(11):1319–23.

56. Martinowich K, Hattori D, Wu H, Fouse S, He F, Hu Y, et al. DNA Methylation-Related Chromatin Remodeling in Activity-Dependent *Bdnf* Gene Regulation. Science (80-). 2003 Oct 31;302(5646):890–3.

57. Duke CG, Kennedy AJ, Gavin CF, Day JJ, Sweatt JD. Experience-dependent epigenomic reorganization in the hippocampus. Learn Mem. 2017 Jul 15;24(7):278–88.

58. Halder R, Hennion M, Vidal RO, Shomroni O, Rahman R-U, Rajput A, et al. DNA methylation changes in plasticity genes accompany the formation and maintenance of memory. Nat Neurosci. 2016 Jan 14;19(1):102–10.

59. Levenson JM, Roth TL, Lubin FD, Miller CA, Huang I-C, Desai P, et al. Evidence That DNA (Cytosine-5) Methyltransferase Regulates Synaptic Plasticity in the Hippocampus. J Biol Chem. 2006 Jun;281(23):15763–73.

60. Miller CA, Sweatt JD. Covalent Modification of DNA Regulates Memory Formation. Neuron. 2007 Mar;53(6):857–69.

61. Tremblay MW, Jiang Y. DNA Methylation and Susceptibility to Autism Spectrum Disorder. Annu Rev Med. 2019 Jan 27;70(1):151–66.

62. Nishioka M, Bundo M, Kasai K, Iwamoto K. DNA methylation in schizophrenia: progress and challenges of epigenetic studies. Genome Med. 2012;4(12):96.

63. Bali P, Im H-I, Kenny PJ. Methylation, memory and addiction. Epigenetics. 2011 Jun 27;6(6):671–4.

64. Irier HA, Jin P. Dynamics of DNA Methylation in Aging and Alzheimer's Disease. DNA Cell Biol. 2012 Oct;31(S1):S-42-S-48.

65. Pellegrini C, Pirazzini C, Sala C, Sambati L, Yusipov I, Kalyakulina A, et al. A Meta-Analysis of Brain DNA Methylation Across Sex, Age, and Alzheimer's Disease Points for Accelerated Epigenetic Aging in Neurodegeneration. Front Aging Neurosci. 2021 Mar 11;13.

66. Shireby G, Dempster EL, Policicchio S, Smith RG, Pishva E, Chioza B, et al. DNA methylation signatures of Alzheimer's disease neuropathology in the cortex are primarily driven by variation in non-neuronal cell-types. Nat Commun. 2022 Sep 24;13(1):5620.

67. Lewis FT. The significance of the term Hippocampus. J Comp Neurol. 1923 Apr;35(3):213–30.

68. Moser M-B, Moser EI. Functional differentiation in the hippocampus. Hippocampus. 1998;8(6):608–19.

69. Seok J-W, Cheong C. Functional dissociation of hippocampal subregions

corresponding to memory types and stages. J Physiol Anthropol. 2020 Dec 2;39(1):15.

70. Anand K, Dhikav V. Hippocampus in health and disease: An overview. Ann Indian Acad Neurol. 2012;15(4):239.

71. Tamnes CK, Bos MGN, van de Kamp FC, Peters S, Crone EA. Longitudinal development of hippocampal subregions from childhood to adulthood. Dev Cogn Neurosci. 2018 Apr;30:212–22.

72. Lee JK, Johnson EG, Ghetti S. Hippocampal Development: Structure, Function and Implications. In: The Hippocampus from Cells to Systems. Cham: Springer International Publishing; 2017. p. 141–66.

73. Manuel Sánchez DM, Limón D, Silva Gómez AB. Obese male Zucker rats exhibit dendritic remodeling in neurons of the hippocampal trisynaptic circuit as well as spatial memory deficits. Hippocampus. 2022 Nov 30;32(11–12):828–38.

74. Yang B, Sanches-Padilla J, Kondapalli J, Morison SL, Delpire E, Awatramani R, et al. Locus coeruleus anchors a trisynaptic circuit controlling fear-induced suppression of feeding. Neuron. 2021 Mar;109(5):823-838.e6.

75. Stepan J, Dine J, Eder M. Functional optical probing of the hippocampal trisynaptic circuit in vitro: network dynamics, filter properties, and polysynaptic induction of CA1 LTP. Front Neurosci. 2015 May 6;9.

76. Squire LR, Stark CEL, Clark RE. THE MEDIAL TEMPORAL LOBE. Annu Rev Neurosci. 2004 Jul 21;27(1):279–306.

77. Auhustinack J, Helmer K, Huber KE, Kakunoori S, Zöelli L, Fischl B. Direct visualization of the perforant pathway in the human brain with ex vivo diffusion tensor imaging. Front Hum Neurosci. 2010;4.

78. Witter MP. The perforant path: projections from the entorhinal cortex to the dentate gyrus. In: Progress in Brain Research. 2007. p. 43–61.

79. van Strien NM, Cappaert NLM, Witter MP. The anatomy of memory: an interactive overview of the parahippocampal–hippocampal network. Nat Rev Neurosci. 2009 Apr;10(4):272–82.

80. Basu J, Siegelbaum SA. The Corticohippocampal Circuit, Synaptic Plasticity, and Memory. Cold Spring Harb Perspect Biol. 2015 Nov 2;7(11):a021733.

81. Cenquizca LA, Swanson LW. Spatial organization of direct hippocampal field CA1 axonal projections to the rest of the cerebral cortex. Brain Res Rev. 2007 Nov;56(1):1–26.

82. Tulving E, Markowitsch HJ. Episodic and declarative memory: Role of the hippocampus. Hippocampus. 1998;8(3):198–204.

83. Bird CM, Burgess N. The hippocampus and memory: insights from spatial processing. Nat Rev Neurosci. 2008 Mar;9(3):182–94.

84. Nunn JA, Graydon FJX, Polkey CE, Morris RG. Differential spatial memory impairment after right temporal lobectomy demonstrated using temporal titration. Brain. 1999 Jan;122(1):47–59.

85. Cave CB, Squire LR. Equivalent impairment of spatial and nonspatial memory following damage to the human hippocampus. Hippocampus. 1991 Jul 3;1(3):329–40.

86. Burgess N, Maguire EA, O'Keefe J. The Human Hippocampus and Spatial and Episodic Memory. Neuron. 2002 Aug;35(4):625–41.

87. Savage L, Buzzetti RA, Ramirez DR. The effects of hippocampal lesions on learning, memory, and reward expectancies. Neurobiol Learn Mem. 2004 Sep;82(2):109–19.

88. Denninger JK, Smith BM, Kirby ED. Novel Object Recognition and Object Location Behavioral Testing in Mice on a Budget. J Vis Exp. 2018 Nov 20;(141).

89. Harrison FE, Hosseini AH, McDonald MP. Endogenous anxiety and stress responses in water maze and Barnes maze spatial memory tasks. Behav Brain Res. 2009 Mar;198(1):247–51.

90. Wenk GL. Assessment of Spatial Memory Using the Radial Arm Maze and Morris Water Maze. Curr Protoc Neurosci. 2004 Jan;26(1).

91. Bizon J, Prescott S, Nicolle MM. Intact spatial learning in adult Tg2576 mice. Neurobiol Aging. 2007 Mar;28(3):440–6.

92. D'Hooge R, De Deyn PP. Applications of the Morris water maze in the study of learning and memory. Brain Res Rev. 2001 Aug;36(1):60–90.

93. Kraeuter A-K, Guest PC, Sarnyai Z. The Y-Maze for Assessment of Spatial Working and Reference Memory in Mice. Methods Mol Biol. 2019;1916:105–11.

94. Vorhees C V., Williams MT. Assessing Spatial Learning and Memory in Rodents. ILAR J. 2014 Jan 1;55(2):310–32.

95. Garcia-Alvarez G, Shetty MS, Lu B, Yap KAF, Oh-Hora M, Sajikumar S, et al. Impaired spatial memory and enhanced long-term potentiation in mice with forebrain-specific ablation of the Stim genes. Front Behav Neurosci. 2015 Jul 14;9.

96. Tsien JZ, Huerta PT, Tonegawa S. The Essential Role of Hippocampal CA1 NMDA Receptor–Dependent Synaptic Plasticity in Spatial Memory. Cell. 1996 Dec;87(7):1327–38.

97. Phasuk S, Jasmin S, Pairojana T, Chang H-K, Liang K-C, Liu IY. Lack of the peroxiredoxin 6 gene causes impaired spatial memory and abnormal synaptic plasticity. Mol Brain. 2021 Apr 19;14(1):72.

98. Wu Y, Zhang J, Peng B, Tian D, Zhang D, Li Y, et al. Generating viable mice with heritable embryonically lethal mutations using the CRISPR-Cas9 system in two-cell embryos. Nat Commun. 2019 Jun 28;10(1):2883.

99. Kim H, Kim M, Im S-K, Fang S. Mouse Cre-LoxP system: general principles to determine tissue-specific roles of target genes. Lab Anim Res. 2018;34(4):147.

100. McLellan MA, Rosenthal NA, Pinto AR. Cre-loxP-Mediated Recombination: General Principles and Experimental Considerations. Curr Protoc Mouse Biol. 2017 Mar;7(1):1–12.

101. Stoller JZ, Degenhardt KR, Huang L, Zhou DD, Lu MM, Epstein JA. Cre reporter mouse expressing a nuclear localized fusion of GFP and β-galactosidase reveals new derivatives of Pax3-expressing precursors. genesis. 2008 Apr;46(4):200–4.

102. Tsien JZ, Chen DF, Gerber D, Tom C, Mercer EH, Anderson DJ, et al. Subregion- and Cell Type–Restricted Gene Knockout in Mouse Brain. Cell. 1996 Dec;87(7):1317–26.

103. Burgin K, Waxham M, Rickling S, Westgate S, Mobley W, Kelly P. In situ hybridization histochemistry of Ca2+/calmodulin-dependent protein kinase in developing rat brain. J Neurosci. 1990 Jun 1;10(6):1788–98.

104. Schwarz SD, Grundbacher E, Hrovat AM, Xu J, Kuśnierczyk A, Vågbø CB, et al. Inducible TDG knockout models to study epigenetic regulation. F1000Research.

2020 Oct 19;9:1112.

105. Hurst JL, West RS. Taming anxiety in laboratory mice. Nat Methods. 2010 Oct 12;7(10):825–6.

106. Wang X, Zhang C, Szabo G, Sun Q-Q. Distribution of CaMKIIα expression in the brain in vivo, studied by CaMKIIα-GFP mice. Brain Res. 2013;1518:9–25.

107. Lezak KR, Missig G, Carlezon Jr WA. Behavioral methods to study anxiety in rodents. Dialogues Clin Neurosci. 2017 Jun 30;19(2):181–91.

108. Sturman O, Germain P-L, Bohacek J. Exploratory rearing: a context- and stress-sensitive behavior recorded in the open-field test. Int J Biol Stress. 2018;21(5):443–52.

109. Lueptow LM. Novel Object Recognition Test for the Investigation of Learning and Memory in Mice. J Vis Exp. 2017;

110. Bach ME, Barad M, Son H, Zhou M, Lu Y-F, Shih R, et al. Age-related defects in spatial memory are correlated with defects in the late phase of hippocampal long-term potentiation in vitro and are attenuated by drugs that enhance the cAMP signaling pathway. Proc Natl Acad Sci. 1999;96(9):5280–5.

111. Jacquot S, Chartoire N, Piguet F, Hérault Y, Pavlovic G. Optimizing PCR for Mouse Genotyping: Recommendations for Reliable, Rapid, Cost Effective, Robust and Adaptable to High-Throughput Genotyping Protocol for Any Type of Mutation. Curr Protoc Mouse Biol. 2019 Dec 26;9(4).

112. Sharma S, Zhu J. Immunologic Applications of Conditional Gene Modification Technology in the Mouse. Curr Protoc Immunol. 2014 Apr 3;105(1).

113. Gusel'nikova V V, Korzhevskiy DE. NeuN As a Neuronal Nuclear Antigen and Neuron Differentiation Marker. Acta Naturae. 2015;7(2):42–7.

114. Gouveia K, Hurst JL. Improving the practicality of using non-aversive handling methods to reduce background stress and anxiety in laboratory mice. Sci Rep. 2019 Dec 30;9(1):20305.

115. Gouveia K, Hurst JL. Reducing Mouse Anxiety during Handling: Effect of Experience with Handling Tunnels. PLoS One. 2013 Jun 20;8(6):e66401.

116. Bailey KR, Crawley JN. Anxiety-Related Behaviors in Mice. 2009.

117. Brown RE, Stanford L, Schellinck HM. Developing Standardized Behavioral Tests for Knockout and Mutant Mice. ILAR J. 2000 Jan 1;41(3):163–74.

118. Bats S, Thoumas J., Lordi B, Tonon M., Lalonde R, Caston J. The effects of a mild stressor on spontaneous alternation in mice. Behav Brain Res. 2001 Jan;118(1):11–5.

119. Alberini CM. Transcription Factors in Long-Term Memory and Synaptic Plasticity. Physiol Rev. 2009 Jan;89(1):121–45.

120. Bernstein C. DNA Methylation and Establishing Memory. Epigenetics Insights. 2022 Jan 19;15:251686572110724.

121. Bisaz R, Travaglia A, Alberini CM. The Neurobiological Bases of Memory Formation: From Physiological Conditions to Psychopathology. Psychopathology. 2014;47(6):347–56.

122. Blaser R, Heyser C. Spontaneous object recognition: a promising approach to the comparative study of memory. Front Behav Neurosci. 2015 Jul 10;9.

123. Beery AK, Shambaugh KL. Comparative Assessment of Familiarity/Novelty

Preferences in Rodents. Front Behav Neurosci. 2021 Apr 13;15.

124. Yang W, Zhou X, Ma T. Memory Decline and Behavioral Inflexibility in Aged Mice Are Correlated With Dysregulation of Protein Synthesis Capacity. Front Aging Neurosci. 2019 Sep 4;11.

125. Miedel CJ, Patton JM, Miedel AN, Miedel ES, Levenson JM. Assessment of Spontaneous Alternation, Novel Object Recognition and Limb Clasping in Transgenic Mouse Models of Amyloid-β and Tau Neuropathology. J Vis Exp. 2017 May 28;(123).

126. Prieur E, Jadavji N. Assessing Spatial Working Memory Using the Spontaneous Alternation Y-maze Test in Aged Male Mice. BIO-PROTOCOL. 2019;9(3).

127. Leslie JC, Shaw D, Gregg G, McCormick N, Reynolds DS, Dawson GR. Effects of Reinforcement Schedule on Facilitation of Operant Extinction by Chlordiazepoxide. J Exp Anal Behav. 2005 Nov;84(3):327–38.

128. Curzon P, Rustay NR, Browman KE. Cued and Contextual Fear Conditioning for Rodents. Buccafusco JJ, editor. Boca Raton: CRC Press/Taylor & Francis; 2009.

129. Olton DS, Samuelson RJ. Remembrance of places passed: Spatial memory in rats. J Exp Psychol Anim Behav Process. 1976 Apr;2(2):97–116.

Appendix

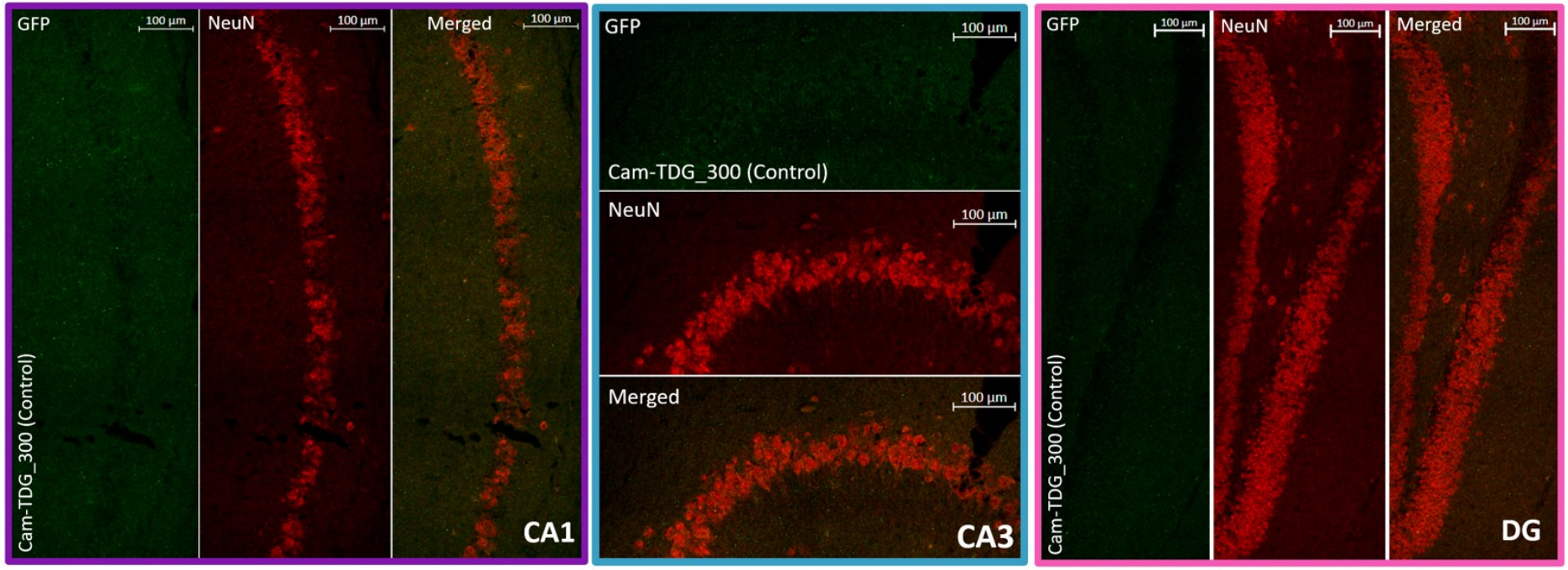

Figure 13. Hippocampal GFP expression in LoxP-miniTdg mice brain tissue. The images show Cre-Induced GFP expression in a LoxP-mini*Tdg* mouse (control), which is indicated by green fluorescence. The images show Cre-induced GFP expression and NeuN expression (red fluorescence) in CA1 highlighted with a purple square, CA3 highlighted with a blue square, and DG highlighted with a pink square. Images were processed in Zen software (Zeiss).

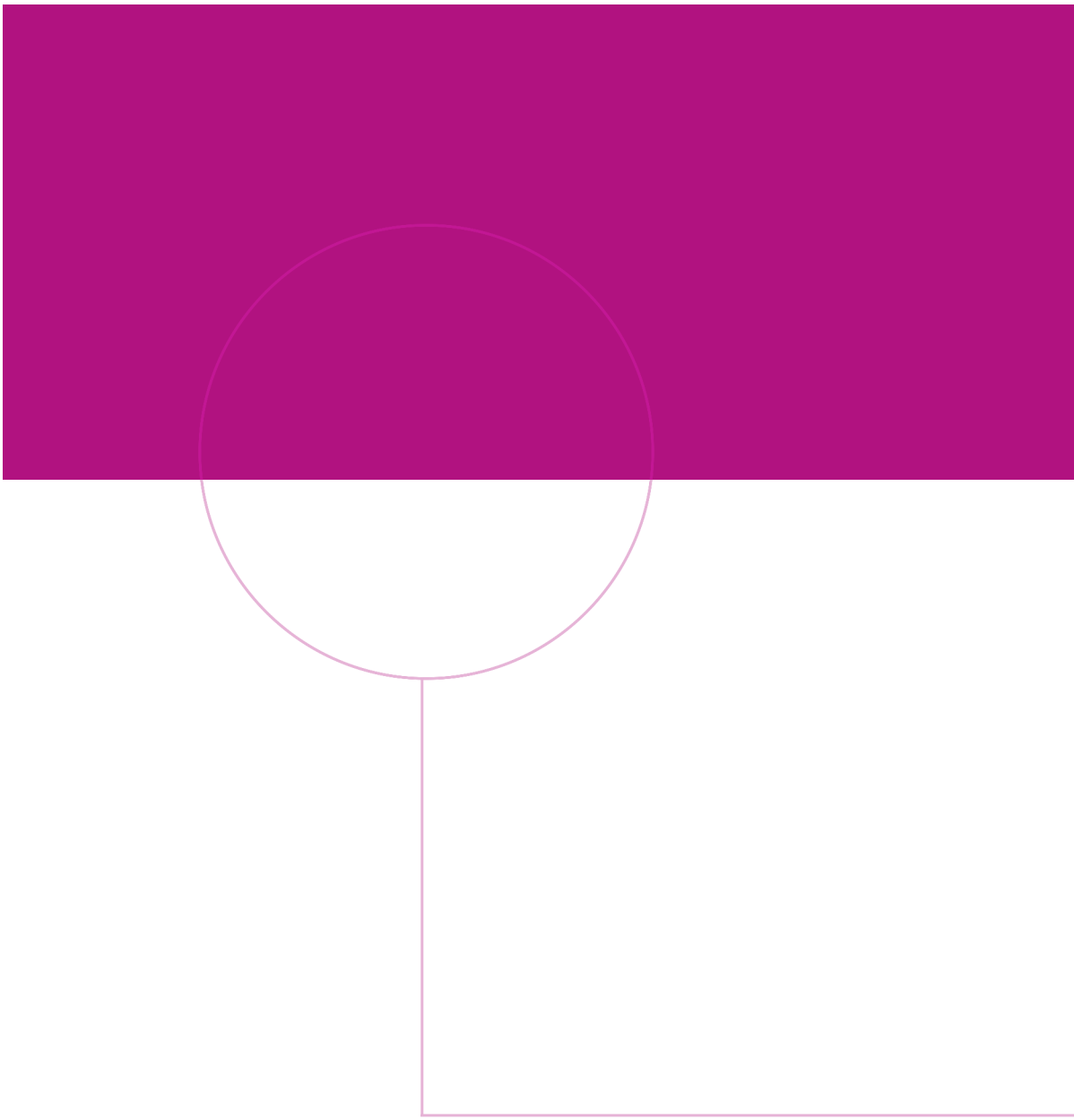

NTNU

Norwegian University of
Science and Technology